Brain Pathology ISSN 1015-6305

MINI-SYMPOSIUM: Pathology & Genetics of (non-CAA) Cerebral Microvascular Disease

CADASIL and CARASIL

Saara Tikka[1]*; Marc Baumann[1]*; Maija Siitonen[2]; Petra Pasanen[2]; Minna Pöyhönen[3]; Liisa Myllykangas[8] Matti Viitanen[4,5]; Toshio Fukutake[6]; Emmanuel Cognat[7]; Anne Joutel[7†]; Hannu Kalimo[8,9†]

[1] Protein Chemistry Unit, Institute of Biomedicine/Anatomy, University of Helsinki, Helsinki, Finland.
[2] Department of Medical Biochemistry and Genetics, Institute of Biomedicine, University of Turku, Turku, Finland.
[3] Department of Clinical Genetics, Helsinki University Hospital, HUSLAB, Helsinki, Finland.
[4] Turku City Hospital, Turku, Finland.
[5] Division of Clinical Geriatrics, Department of Neurobiology, Care Sciences and Society, Karolinska Institutet, Stockholm, Sweden.
[6] Department of Neurology, Kameda Medical Center, Kamogawa, Chiba, Japan.
[7] INSERM, U1161 and Université Paris Diderot, Sorbonne Paris Cité, UMRS 1161, Paris, France.
[8] Department of Pathology, Haartman Institute, University of Helsinki, Helsinki, Finland.
[9] Institute of Biomedicine, Department of Forensic Medicine, University of Turku, Turku, Finland.

Keywords
CADASIL, CARASIL.

Corresponding author:
Hannu Kalimo, MD, PhD, Institute of Biomedicine, Department of Forensic Medicine, University of Turku, FI-20520, Turku, Finland
(E-mail: *hannu.kalimo@helsinki.fi*)

Received 21 July 2014
Accepted 28 July 2014

* shared first authorship
† shared senior authorship

doi:10.1111/bpa.12181

Abstract

CADASIL and CARASIL are hereditary small vessel diseases leading to vascular dementia. CADASIL commonly begins with migraine followed by minor strokes in mid-adulthood. Dominantly inherited CADASIL is caused by mutations (n > 230) in *NOTCH3* gene, which encodes Notch3 receptor expressed in vascular smooth muscle cells (VSMC). Notch3 extracellular domain (N3ECD) accumulates in arterial walls followed by VSMC degeneration and subsequent fibrosis and stenosis of arterioles, predominantly in cerebral white matter, where characteristic ischemic MRI changes and lacunar infarcts emerge. The likely pathogenesis of CADASIL is toxic gain of function related to mutation-induced unpaired cysteine in N3ECD. Definite diagnosis is made by molecular genetics but is also possible by electron microscopic demonstration of pathognomonic granular osmiophilic material at VSMCs or by positive immunohistochemistry for N3ECD in dermal arteries.

In rare, recessively inherited CARASIL the clinical picture and white matter changes are similar as in CADASIL, but cognitive decline begins earlier. In addition, gait disturbance, low back pain and alopecia are characteristic features. CARASIL is caused by mutations (presently n = 10) in high-temperature requirement. A serine peptidase 1 (*HTRA1*) gene, which result in reduced function of HTRA1 as repressor of transforming growth factor-β (TGF β) -signaling. Cerebral arteries show loss of VSMCs and marked hyalinosis, but not stenosis.

INTRODUCTION

The acronyms CADASIL and CARASIL—two hereditary small vessel diseases (SVD)—differ from each other only by D vs. R (cerebral autosomal dominant vs. recessive arteriopathy with subcortical infarcts and leukoencephalopathy), which may confuse at least those who less actively follow the SVD literature. The acronyms imply a difference only in the mode of inheritance—dominant vs. recessive—however, their gene defects, clinical pictures, imaging findings and pathologies do differ from each other to such an extent that alert clinicians, radiologists and pathologists should be able to distinguish these two SVD entities, the definite diagnoses of which would then emerge at the latest in molecular genetic analyses. In this article, we describe first for CADASIL and thereafter for CARASIL the basic clinical findings, genetics, biochemistry, pathologies and suggested pathogeneses of these two entities with some similarities but at the same time major differences. Finally, the present situation of and prospects for evidence-based therapeutics is discussed.

HISTORY

The first CADASIL family—later verified by genetic analysis of old tissue specimens—was reported by van Bogaert as "hereditary Binswanger's disease" in 1955 (128). Thereafter, the disease entities resembling the present CADASIL received many different names (e.g. chronic familial vascular encephalopathy, Familiare zerebrale Arteriosklerose, Familiäre zerebrale Gefässerkrankung, familial disorder with subcortical ischemic strokes, dementia and leukoencephalopathy and familial Binswanger's syndrome). With the knowledge of that time, it is not surprising that CARASIL (also known as Maeda syndrome) in 1960 was described by Nemoto similarly as a form of Binswanger syndrome and then published by Maeda *et al* in 1976 (81) as multifocal softenings in the cerebral white matter caused by cerebral angiitis (Binswanger's disease). The discovery of the causative gene defects then finally and definitely specified these two SVDs: For CADASIL, the linkage to chromosome 19 was identified in 1993 (125) and the causative *NOTCH3* gene on 19p13 was discovered in 1996 (54). For

CARASIL, the defective *HTRA1* gene on chromosome 10q25 was determined in 2009 (45).

EPIDEMIOLOGY

CADASIL

After the gene defect of CADASIL was established and doctors became better aware of this entity, the number of both reported and diagnosed cases increased rapidly. At present, CADASIL is the most common hereditary vascular dementia and it has been reported in all ethnic groups from Far West to Far East. However, exact surveys of its prevalence are few. In west Scotland, the prevalence of patients with definite diagnosis in 2005 was 1.98/100 000 and that of predicted mutation carriers was 4.14/100 000 (105). In Northeast England, in an outbred Western European population, the minimum prevalence for definite cases in 2012 was 1.32/100 000 (95). In geographic locations, where the population has a more limited genetic background, such as Finland and Gran Canaria island, ancestor phenomena and/or exceptionally high prevalences have been recorded. In Finland (population about 5 million), the dominant mutation p.Arg133Cys was introduced in the late 1600s or early 1700s (93), the prevalence being about 4/100 000. The ancestor effect is still more striking on the island of Gran Canaria, where the prevalence reaches 14/100 000 (121 patients with p.Arg207Cys mutation in a population of about 900 000; Drs. A Santana and J Delgado, pers. comm.). In Canada and United States, the prevalence numbers have been surprisingly low (in most Canadian provinces < 1/100 000, Dr. V Saly, pers. comm.) considering the high standard of neurology in those countries. Another approach by analyzing the number of CADASIL cases among patients with lacunar infarcts and leukoaraiosis gave frequencies of 11% (one out of nine) for patients under 50 years and 2% (one out of 48) for patients under 65 years of age (32). In a Korean study of 151 consecutive acute ischemic strokes (mean age 70 years), 4.0% (n = 6) were diagnosed to suffer from CADASIL (21). The percentages might be somewhat higher, as these two last mentioned studies used only a limited screening test for *NOTCH3* mutations.

CARASIL

CARASIL is a very rare disease. Until recently, only somewhat over 50 cases have been reported (39, 97), 48 from Japan, three from China (19, 131) and one case each from Spain (83), Romania (9) and Turkey (8). With the growing awareness also outside the far eastern countries, more families are expected to be diagnosed and reported.

GENETICS AND BIOCHEMISTRY

CADASIL

CADASIL is—as its name implies—autosomally dominantly inherited, and only a few patients with definite *de novo* mutations have been reported (55). The defective gene is *NOTCH3* in 19p13.1–13.2. The 33 exons of *NOTCH3* encode a single pass transmembrane heterodimer receptor protein Notch3 (N3) comprising 2321 amino acids. Similarly, as all Notch receptors, Notch3 is synthesized as a full-length protein (Figure 1), which is subsequently proteolytically cleaved (S1 cleavage) by furin into two parts. The N-terminal extracellular domain (N3ECD, 210 kDa) is composed of 34 epidermal growth factor-like repeats (EGFr), each of which encompasses six cysteine residues, followed by three

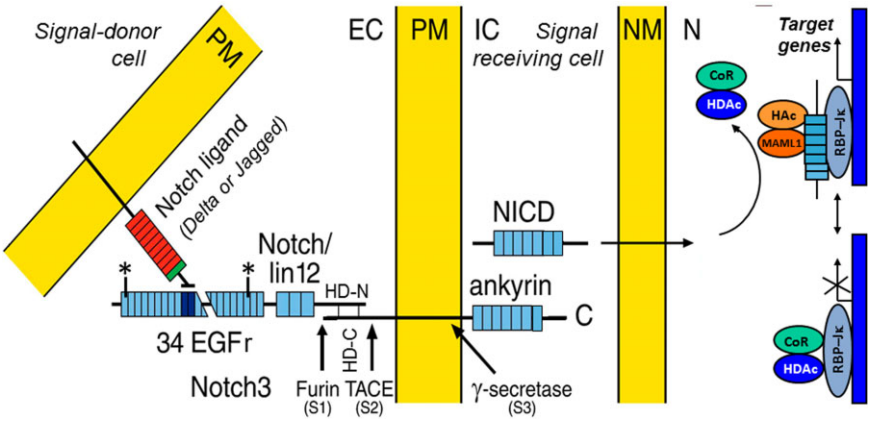

Figure 1. A schematic presentation of Notch signaling. Notch3 is constitutively cleaved by furin (S1) and the bipartite molecule is inserted to the plasma membrane (PM). The extracellular domain (N3ECD) consists of 34 epidermal growth factor (EGF)-like repeats, followed by three notch/lin-12 repeats, a transmembrane domain and an intracellular domain (NICD), which contains seven ankyrin repeats. The binding site of the ligand (in human Delta or Jagged) is at EGF repeats 10–11. Upon binding, N3ECD is cleaved external to the intramembranous domain (S2). Thereafter occurs the intramembranous S3 cleavage and NICD enters the nucleus to release the repressor molecules CoR and HDAc, and it binds to a transcription regulator of CSL family, RBP-Jκ, and activates transcription. CADASIL mutations are in EGF repeats 1–32 (exons 2–23) between the asterisks. EC = extracellular space, IC = intracellular space, NM = nuclear membrane, N = nucleus, TACE = tumor necrosis factor α-converting enzyme, HD = heterodimerization domain, CoR and HDAc = repressors, HAc and MAML1 = components of an activation complex.

Notch/Lin12 repeats. At the heterodimerization domains (HD-N and HD-C), N3ECD is non-covalently connected to the 97 kDa C-terminal part, which comprises a transmembrane (N3TMD) and an intracellular domain (N3ICD; together N3TMIC). N3ICD contains seven ankyrin repeats (Figure 1).

Notch3 belongs to the Notch family (four members in mammals), whose signaling pathways are indispensable during development of most organs. Their importance is reflected by the presence of orthologous genes with high degree of homology from nematodes to man. Notch repertoire during organogenesis, including vasculogenesis, covers for example stem cell renewal, cell proliferation, determination of cell fate and differentiation and apoptosis. The exact function of Notch3 is not known in adult humans, in whom Notch3 is expressed predominantly in VSMCs (56, 103), the molecular phenotype and metabolic characteristics of which cells appear to be different in different vascular beds (for details see succeeding sections).

The Delta/Serrate/Lag-2 (DSL) ligands of Notch receptors belong to the Delta-like family (DLL1, 3 and 4) and Serrate family Jagged (Jag 1 and 2). They have similar molecular structure as Notch receptors, that is they are transmembrane proteins, the extracellular domain of which contains several EGFrs. Although both the ligands and Notch receptors are presented on the surface of vascular smooth muscle cells (VSMC), the ligands transactivate Notch receptor on the neighboring cells, whereas Notch receptors expressed on the same cell are cis-inhibited (35). The ligand-binding site in Notch3 is at EGFr 10–11. Upon binding of its ligand, N3ECD is non-enzymatically dissociated from the heterodimeric Notch3 and the bound ligand and N3ECD are transendocytosed into the ligand-expressing cell. Thereby the membrane-bound C-terminal part of Notch3 (composed of N3TMD and N3ICD) becomes exposed for cleavage by ADAM10 or by ADAM17 (also known as TNF-alpha converting enzyme; TACE) just outside the plasma membrane (S2 cleavage), whereafter the final S3 cleavage by γ-secretase (the same enzyme as in Alzheimer's disease) can occur within the membrane to detach N3ICD from N3TMD (11, 96). The transendocytosed non-mutated N3ECD is degraded in the ligand-presenting cell. N3ICD enters the nucleus of the receptor-presenting cell and interacts with RBP-Jκ and co-activators to activate transcription of its target genes (37, 38) (Figure 1).

The pathogenic mutations—so far over 230 different reported—are located in exons 2–24 in the N3ECD, with prominent clustering in exons 3 and 4 encoding EGFr 2–5 (over 40% of mutations in over 70% of families occur in these exons). A great majority of mutations (>95%) are missense mutations, which cause either substitution of a wild type (wt) cysteine with another amino acid or vice versa. In addition, eight different deletions, two duplications (70, 82) and two splice site mutations (57, 112) have been reported. Remarkably, all these mutations result in an uneven number of cysteine residues in the affected EGFr, which situation appears to be crucial in the pathogenesis of CADASIL. However, at least 11 patients/families, whose clinical picture was considered compatible with CADASIL and who carried a non-cysteine mutation in *NOTCH3*, have been reported. Besides, we have been consulted about several such patients. Whether the CADASIL-like disease in these patients has a causal relationship with the non-cysteine *NOTCH3* mutation has been debated and remains to be investigated (23, 24, 88) (see also Pathogenesis section).

At present, five patients with homozygous cysteine mutations in NOTCH3 [Tuominen *et al*: p.Arg133Cys (126), Liem *et al*: p.Arg578Cys (78), Ragno *et al*: p.Gly528Cys (104), Soong *et al*: p.Arg544Cys (118) and Vinciguerra *et al*: p.Cys183Ser (130)] have been reported.

CARASIL

Analogously, CARASIL is—as its name implies—autosomally recessively inherited and, thus, mutations on both alleles, either homozygous or compound heterozygous, are required to cause the disease.

The gene defect of CARASIL was discovered collaboratively by a large Japanese group of researchers directed by Professors O. Onodera and S. Tsuji, the majority of the participants being based at Niigata University (45). Five families with clinical CARASIL were enrolled and they were first analyzed by genome-wide linkage and thereafter the defective gene was fine mapped to a 2.4-Mb region on chromosome 10q. High-temperature requirement A serine peptidase 1 (*HTRA1*) was selected as a candidate gene because it is expressed in the blood vessels, skin and bone. *HTRA1* in human is composed of nine exons encoding a protein consisting of 480 residues and comprising four functional domains (Figure 2). The exons 3–6 encode the main domain of a trypsin-like serine protease that represses signaling by transforming growth factor-β (TGF-β) family members (45).

The sequence analysis by Hara *et al* (45) revealed in the serine protease domain of *HTRA1* four homozygous mutations: two missense and two nonsense mutations (Table 1 and Figure 2), which were not discovered in 125 controls. Thereafter (at least), four novel missense mutations have been reported and among them the first Caucasian patient (83) (Table 1). Another Caucasian patient from Turkey (8) carried the same nonsense mutation as one of the original families of Hara *et al* (45). The first and only reported compound heterozygous patient was also Caucasian (9) (Table 1); this individual carried a classic missense mutation in exon 4 of *HTRA1* paired with an exceptional single nucleotide deletion in exon 1 that causes a frameshift.

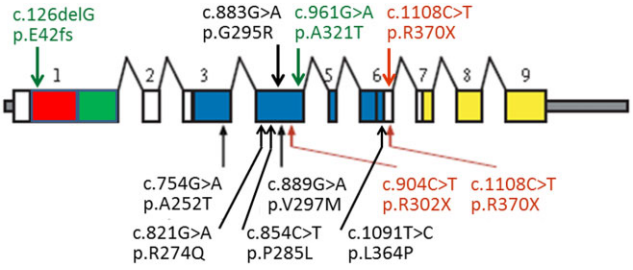

Figure 2. A schematic presentation of *HTRA1* mutations. The mutations reported in Far-Eastern patients are presented below the gene and those in Caucasian patients are presented above the gene. Missense mutations are presented in black, nonsense mutations in red and the compound heterozygous mutation in green. [Domains of *HTRA1*. Red: Insulin-like growth factor binding protein domain. Green: Kazai-type serine protease inhibitor domain. Blue: Trypsin-like serine protease domain. Yellow: PDZ domain. Scheme modified after Hara *et al* (45); for details see Table 1].

Table 1. CARASIL mutations. Abbreviations: homoz = homozygous; heteroz = heterozygous; ms = missense; ns = nonsense; del = deletion.

E	Mutation type	Nucleotide	Protein	Ethnicity	Publication
Far-Eastern patients					
3	homoz, ms	c.754G > A	p.Ala252Thr	Japanese	Hara *et al N Engl J Med* 2009; **360**: 1729–1739. (45)
4	homoz, ms	c.889G > A	p.Val297Met		
4	homoz, ns	c.904C > T	p.Arg302X		
6	homoz, ns	c.1108C > T	p.Arg370X		
4	homoz, ms	c.821G > A	p.Arg274Gln	Japanese	Nishimoto *et al Neurology* 2011; **76**:1353–1355.
4	homoz, ms	c.854C > T	p.Pro285Leu	Chinese	Chen *et al J Int Med Res* 2013; **41**:1445–1455. (19)
6	homoz, ms	c.1091T > C	p.Leu364Pro	Chinese	Wang *et al CNS Neurosci Ther* 2012; **18**: 867–869. (131)
Caucasian patients					
4	homoz, ms	c.883G > A	p.Gly295Arg	Spanish	Mendioroz *et al Neurology*; 2010; **75**: 2033–2035. (83)
6	homoz, ns	c.1108C > T	p.Arg370X	Turkish	Bayrakli *et al Turk Neurosurg* 2014; **24**:67–69. (8)
1	compound heteroz, del & ms	c.126delG &	p.Glu42fs &	Romanian	Bianchi *et al Neurology* 2014; **82**:898–900. (9)
4		c.961G > A	p.Ala321Thr		

HTRA1 belongs to the family of high-temperature requirement A serine proteases, which in mammals participates in a variety of physiological processes, such as cell signaling and protein degradation, and is associated with development of the musculoskeletal system. For CARASIL, important repression of TGF-β signaling occurs as follows (97, 116, 124): TGF-β1 is synthesized as a pre-pro-protein. In the endoplasmic reticulum, proTGF-β1 is dimerized and in trans-Golgi network (TGN), proTGF-β1 is then cleaved by furin convertase. The two cleaved products of proTGF-β1, latency-associated peptide (LAP) and the mature TGF-β1 peptide, are connected non-covalently to yield a small latent TGF-β1 complex. This small latent TGF-β1 complex is bound to LTBP1 by LAP forming the large latent TGF-β1 complex, which complex is secreted and sequestered in the extracellular matrix (ECM). Different proteases/integrins in the ECM can cleave LAP to release the mature TGF-β, which then can bind to its receptors. HTRA1 represses TGF-β signaling by cleaving proTGF-β1 in the endoplasmic reticulum (ER) and the cleaved products are degraded by ER-associated protein degradation (ERAD), resulting in the reduction of mature TGF-β1.

Hara *et al* (45) demonstrated that both missense mutations and one nonsense mutation (p.Arg302X) resulted in protein products with clearly lowered protease activity by 21%–50%, which was not enough to repress signaling by the TGF-β family, whereas the other nonsense mutation (p.Arg370X) caused loss of HTRA1 protease activity by nonsense mediated decay of mRNA. Upregulated TGF-β signaling is known to result in increased synthesis of ECM proteins with consequent vascular fibrosis (71). Both immunohistochemical analysis and *in situ* hybridization of the cerebral small arteries in CARASIL patients showed increased expression of fibronectin and versican in the thickened tunica intima and of TGF-β1 in the tunica media.

CLINICAL PICTURES

Even though the gene defects are known, the exact pathogenesis, that is the mechanisms by which the defective pathogenic genes cause these two SVDs are still to be discovered. In spite of that, we have now an effective arsenal of both knowledge and machinery to diagnose these patients.

Clinical picture of CADASIL

As the clinical picture of CADASIL has been described in detail in several excellent reviews (2, 18, 28, 61, 62, 101), only a short summary of the clinical findings—relevant to the theme of this mini-symposium—is described. The wide variability of the clinical picture, also between family members with the same mutation and even between monozygotic twins (94), is repeatedly emphasized.

There is a relative lack of classic vascular risk factors, but for example arterial hypertension, hypercholesterolemia, smoking and diabetes mellitus are known to impact on CADASIL patients (2, 18, 28, 61, 62, 117). The four cardinal manifestations are:

(i) *Migraine with aura:* About 20%–40% of CADASIL patients manifest with this symptom, while up to 60% suffer from migrainous headache without aura. The average age of onset is around 30 years of age, although it may appear even before the age of 10 years, for example (18, 43), and besides, the aura may be exceptionally severe, for example (2, 18, 28, 43, 61, 129). Remarkably, in female patients, late pregnancy or puerperium often elicits their first attack of migraine with aura or aggravates such attacks (108).

(ii) *Ischemic attacks:* Ischemic strokes, often preceded by transient ischemic attacks (TIA, which are difficult to distinguish from severe migrainous aura) are the most common (up to 85% of symptomatic patients) manifestations. The age of first-ever stroke varies vastly. The youngest reported patient with stroke was only 11 years of age (43), whereas some exceptional patients do not suffer their first-ever stroke until they have reached their 70th birthday (133) (Miao *et al* unpublished). Such late-onset cases may easily remain undiagnosed being considered "just common old age strokes". The mean ages reported are around 40–50 years (2, 18, 28). The strokes are almost always subcortical and typically present as lacunar syndromes, such as pure motor or sensory deficits, dysarthria-clumsy hand syndrome, expressive dysphasia or visual field defects. Major strokes because of larger infarcts in the supply territories of major cerebral arteries are rare, most likely coincidental, not related to CADASIL.

(iii) *Cognitive decline and dementia:* Impairment in executive function and working memory was recorded already before TIA and strokes. By testing for these two functions and for mental

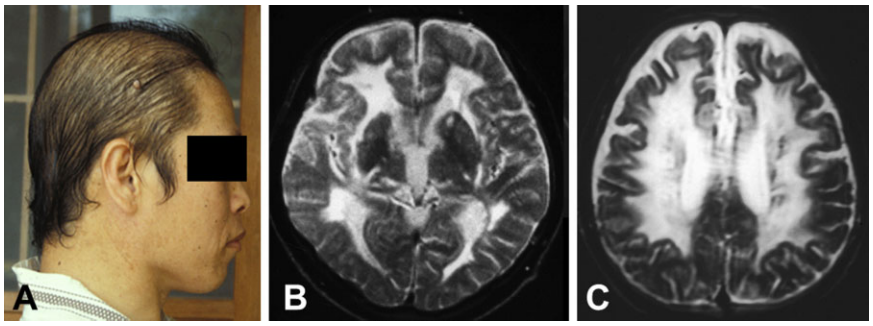

Figure 3. Loss of hair is clearly noticeable already at the age of 34 years in this male CARASIL patient (**A**). At the age of 33 years, T2-weighted MRI disclosed diffuse leukoencephalopathy and lacunes (**B** and **C**).

speed, non-demented mutation carriers could be distinguished from controls. Episodic memory was relatively well preserved until late stage of the disease (3, 27, 101, 120), but eventually the patients develop a serious dementia of subcortical vascular type. (iv) *Psychiatric manifestations:* 20%–30% of CADASIL patients suffer from mood disturbances, the most common and serious being depression, which is expected in patients who have experienced the disease in their family and have an insight of their own disease. Apathy is a very common symptom; up to 41% of patients in a large French CADASIL cohort were apathetic. It appears to correlate with the patients' age, severity of cognitive impairment, other neuropsychiatric symptoms (often depression) and load of subcortical tissue lesions (106). Manic episodes are relatively uncommon (ca. 2%), although CADASIL may sometimes be mistaken for bipolar mood disorder before its true nature is discovered. Additional disturbances have been reported, including schizophrenia, psychosis, paranoia, aggression and dysthymia (14, 18, 28, 129).

Imaging in CADASIL

The imaging findings in SVDs including CADASIL are described in the article by Salamon in this mini-symposium (113). Here, we present a few essential magnetic resonance imaging (MRI) findings [with reference to figures in the article (113)] complemented by selected examinations applying special imaging methods.

White matter hyperintensities (WMHI) in temporopolar region and capsula externa on T2-weighted (T2w) or Fluid-Attenuated Inversion Recovery (FLAIR) MRI have been considered pathognomonic findings in CADASIL [figure 3B in (113)]. These are complemented by periventricular, usually spotty leukoaraiosis, which gradually involves most of the cerebral WM [figure 4 in (113)]. Interestingly, the prominence of the characteristic temporopolar WMHI may depend on the patients' ethnic background, being lesser in Chinese patients (72, 132). These MRI lesions are detectable already in the presymptomatic stage even before the age of 20 years and the youngest reported patient with subcortical foci of increased T2 hyperintensity was only 8 years old (48). The characteristic lacunar infarcts can be visualized in computerized tomography (CT) and in T1w or fluid-attenuation inversion recovery (FLAIR) MRI as areas of decreased signal, predominantly in cerebral WM and deep grey matter (GM) [figure 3A in (113)]. Lacunar infarct lesion load is the most important MRI parameter associated with cognitive dysfunction in CADASIL (77). Occurrence of simultaneous multiple acute infarcts, such as those usually caused by and ascribed to embolization, has been detected in CADASIL by diffusion-weighted MRI (41).

The above-mentioned leukoaraiosis pattern implies a widely distributed diffuse leukoencephalopathy, which by diffusion tensor imaging (DTI) is detected as increased water diffusivity and loss of anisotropy, that is the diffusion of water can occur more freely in any

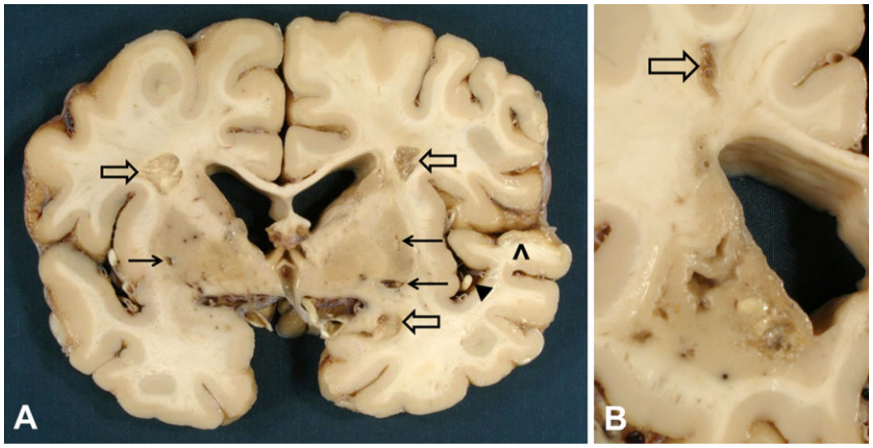

Figure 4. Three old infarcts of moderate size in cerebral white matter (open arrows) and smaller lacunar infarcts in putamen bilaterally (arrows) in a 65-year-old female CADASIL patient with p.Arg133Cys Notch3 mutation. Note the relatively spared cortex except for the ischemic lesion in temporal cortex (arrowhead) because of atherosclerotic occlusion of a middle cerebral artery branch [black triangle; (**A**)]. In this same patient's caudate nucleus, the lesions are more severe than in putamen. In the WM of the centrum semiovale, there is another small cystic infarct [open arrow; (**B**)]. Lateral ventricles in both (**A**) and (**B**) are widened because of ischemic tissue loss.

direction. This indicates accumulation of fluid in enlarged extracellular space (vasogenic/interstitial brain edema) associated with microstructural pathology, myelin and axonal damage (see Histopathology post-mortem section). Corresponding to such tissue damage, DTI results correlate better with the patients' clinical deterioration than T2w images (16). DTI alterations are also detectable in the normal-appearing WM outside the T2w hyperintensities as a harbinger of incipient microstructural abnormalities.

In one-third to two-thirds of CADASIL patients, T2* (gradient echo) MRI discloses small hypointensities, microbleeds [figure 3A in (113)], which represent perivascular accumulations of hemosiderin laden macrophages indicating focal extravasation of red blood cells (Figure 10). Microbleeds are clinically silent and their frequency was not associated with the severity of patient's cognitive dysfunction (73). Microbleeds are primarily located in the cerebral cortex, subcortical WM, basal ganglia and brainstem [figure 3a in (113); all outside ischemic lesions and 82% outside regions that are hyperintense in T2w MRI (29)]. Their frequency increases with patients' age, blood pressure, volume of T2w lesions and antiaggregant therapy (29, 73). Microbleeds are not specific to CADASIL, but they also occur in other SVD of the central nervous system, such as arteriolosclerosis and amyloid angiopathy. They were considered to be largely an independent manifestation of the underlying angiopathy (29). Although direct association has not been reported, concerns that microbleeds may increase the risk of intracerebral hemorrhage have been expressed (73).

As described in the succeeding sections, the brunt of brain pathology targets small arteries and arterioles. However, the arteries and arterioles in SVDs are too small to be specifically visualized by conventional MRI. The application of 7 tesla MRI (10) to *in vivo* visualization of the pathologies developing in small WM arteries in CADASIL and other SVDs will certainly provide interesting new data.

Clinical picture in CARASIL

The clinical features of CARASIL have been described in several articles (39, 40, 97, 136) (and many in Japanese), hence we present here again only an outline. Neurologic symptoms and signs are in many respects similar to those in CADASIL with lack of hypertension having been more explicitly emphasized in some reports on CARASIL (40). Half of the patients experience recurrent ischemic strokes, most often of the lacunar type. These lead to stepwise, progressive impairment of brain functions and finally to dementia, usually by the age of 30 to 40 years. Memory dysfunction in CARASIL appears to be more severe than in CADASIL. An interesting sign—visible to naked eye—is premature diffuse baldness, which predominantly concerns male patients (Figure 3A). Because the connective tissue is also affected in CARASIL, about 80% of the patients suffer from low back pain because of disk herniation and spondylosis deformans, usually between lower thoracic or upper lumbar levels. Cervical spondylosis is also often found.

Imaging in CARASIL

Brain MRI findings are in many respects similar to those in CADASIL (39, 97, 136). In T2w, MRI hyperintensities occur in periventricular and deep WM and sometimes even in anterior temporal WM and capsula externa, as is typical of CADASIL (Figure 3B and C). In CARASIL, the WM changes appear to develop more homogeneously than in CADASIL and the U-fibers are relatively spared. Multiple lacunar infarct are also detected, predominantly in the basal ganglia and thalamus. On spinal MRI, cervical and lumbar spondylosis and disk degeneration become observable around the age of 30 years, often well after the onset of symptoms (97).

CIRCULATORY DISTURBANCES

CADASIL

The reduction of cerebral blood flow (CBF) in CADASIL has been found by applying several different imaging methods, such as positron emission tomography (PET) (15, 127), Doppler sonography (76) and MRI bolus tracking method (12, 17). Corresponding to the imaging findings and the sparing of cerebral cortex (see Pathology of CADASIL section), CBF is first and predominantly reduced in cerebral WM. This was detected by PET already at a presymptomatic stage, although it became more apparent at ages above 30 years, when also the strokes begin to appear. CBF in the cerebral cortex was not reduced until later ages and never to such an extent as in WM. Corresponding to the reduction in CBF, morphological studies have shown definite stenosis of WM arterioles (for details see Pathology of CADASIL section) (84). In a presymptomatic patient, the oxygen extraction fraction (OEF) was shown to increase indicating that the brain thereby attempts to compensate for the decreased CBF by increasing OEF (15). On the other hand, the cerebral metabolic rate of oxygen (CMRO2) (15) and glucose consumption (CMRgluc) (127) were not reduced until later stages parallel to the development of dementia and tissue loss, indicating that the early stage decrease in CBF is because of the arteriopathy instead of being just secondary to tissue loss.

Concordantly, by applying bolus tracking and Doppler methods, CBF and cerebral blood volume (CBV) were found to be reduced within T2w hyperintense areas in the WM, more severely in demented than in non-demented patients (12, 17). Besides, in the normal-appearing WM, a trend of reduced CBV was noticed (17). Furthermore, the hemodynamic reserve is reduced in CADASIL patients because acetazolamide induced a lesser increase in CBF in CADASIL patients' T2w hyperintense WM areas than in control subjects' WM (17). This is well understandable, as CADASIL patients' WM arteries have become stenosed and stiffened by fibrosis (84) (see Pathology of CADASIL section) and thus less responsive to acetazolamide. This may also be the cause of the prolonged arteriovenous cerebral transit time in both disabled and non-disabled CADASIL patients as demonstrated by Liebetrau *et al* (76). Experimental studies have given similar results: transgenic mice expressing p.Arg90Cys-mutant human *NOTCH3* showed reduced responses to hypercapnia and acetazolamide, higher cerebrovascular resistance during hypertension and their lower limit of CBF autoregulation was shifted to higher blood pressures (69).

Retinal vasculature offers an exceptional and excellent *in vivo* view of arterioles. In CADASIL patients, retinal capillary blood flow was found to be mildly to moderately reduced (47). Furthermore, general arterial narrowing and arteriovenous nickings were common. Straightening of the retinal arterioles and a

marked wall reflex occurred and the arterio-venous (A/V) ratio was significantly lower than that in the controls. However, although CADASIL does induce a wide variety of ophthalmologic alterations, these resulted in only minimal functional disturbances and most often in no major ischemic injuries in the retina. Thus, the retina is relatively spared, which conclusion conforms with the results in the cerebral cortex, with which the retina and its arterioles are analogous (109).

As the arteriopathy in CADASIL is generalized, it is not surprising that vasoregulation is disturbed also in the systemic vasculature. Stenborg *et al* (119) showed in the forearm of CADASIL patients that endothelium-dependent vasodilation is impaired in resistance arteries, but not in a large conduit artery, a. brachialis. This impairment results in reductions in both basal and stimulated blood flow. Similarly, Gobron *et al* (42) reported that after the release of forearm cuff occlusion and after nitroglycerin administration, the maximum changes in the diameter of the brachial artery did not differ between patients and controls, whereas skin circulation showed delayed post-occlusive hyperemia response. They concluded that this modified kinetics of skin vasodilation was presumably caused by the structural changes in microvascular VSMCs. Experimental studies have yielded similar results: tail arteries from transgenic mice expressing p.Arg90Cys-mutant human *NOTCH3* showed *in vitro* significantly decreased flow-induced dilation (33).

In spite of the above-described systemic circulatory disturbances and autopsy verified structural involvement of arteries in most organs (110), hardly any clinical manifestations other than the neurological ones have been described. Myocardial infarctions have been reported in a Dutch CADASIL cohort (74), but not in some other studies, for example (14, 26, 28).

Circulatory disturbances in CARASIL

Very few studies on CBF in CARASIL have been published. Reduced CBF has been shown with single photon emission computed tomography (SPECT) and this reduction appeared to be relatively diffusely distributed (40, 115). Since at present there is no animal model for CARASIL, experimental studies on circulatory disturbances in HTRA1-deficient animals have not been published.

PATHOLOGY OF CADASIL

Autopsy findings

Macroscopic findings in CADASIL

In concordance with the imaging findings, the cerebral cortex is relatively spared, whereas multiple small lacunar infarcts are found predominantly in the cerebral WM and deep GM (Figure 4) as well as occasionally also in the brain stem. The severity of the lesions varies considerably between different, even neighboring anatomic regions. Stenoses in large cerebral arteries and rare larger, territorial infarcts (20, 85) have been reported, but they are most likely coincidental insults, not directly related to CADASIL. Besides, because CADASIL does not protect the patients from atherosclerosis, atherosclerotic infarcts may also occur, and these often impact also on cerebral cortex (Figure 4A).

T2*w MRI has shown that microbleeds are relatively common in CADASIL [see Imaging in CADASIL section and figure 3A in (113) and for pathology, Figure 10A–D] and they have been considered predictive for intracerebral hemorrhages (ICH). ICHs have been reported to be significantly associated with microbleeds among Chinese patients with p.Arg544Cys mutation, but on the other hand, these patients were also hypertensive (22). However, compared with the frequency of microbleeds, ICHs are relatively uncommon; just over 20 cases have been reported. Thus, microbleeds do not appear to impose a very serious threat of ICH. It appears that the fibrotic arterioles of CADASIL are less fragile than amyloid laden arteries in cerebral amyloid angiopathy (CAA). A few ICHs have been purely spontaneous, but most often they have occurred in patients, who have been hypertensive and/or treated with anticoagulants or antiaggregants. The majority of ICHs have been located in basal ganglia or thalamus with a few in cerebellum (75, 107).

Histopathology post-mortem

Corresponding to MRI and macroscopic findings, the brunt of histopathology is seen in cerebral WM and deep GM, whereas cortical GM is involved only to a minor extent. Already in routine hematoxylin and eosin-stained sections (Figure 5B), small arteries in cerebral WM appear thick-walled and exceptionally rounded with basophilic (Figure 5B) and PAS-positive (Figure 5C) staining of tunica media. Fibrous connective tissue accumulates in tunica adventitia, which may occasionally result in complete obliteration of arterioles (Figure 5D). Immunohistochemistry (IHC) discloses pathognomonic granular deposits of N3ECD immunopositivity in tunica media (Figure 5E). In parallel, α-smooth muscle actin (α-SMA) positivity decreases indicating degeneration of VSMCs (Figure 5F). In tunica adventitia, various types of collagen (Figure 5G), laminin, clusterin and other ECM proteins accumulate. Although cerebral cortex is relatively spared, N3ECD is also deposited in the tunica media of cortical arteries, but the adventitial thickening is markedly more prominent in WM arterioles (Figure 6A vs. B). Deposition of N3ECD expectedly begins already at the presymptomatic stage (Figure 6C). At advanced stages, N3ECD deposits are discernible also on veins and capillaries in both cerebral WM and GM (Figure 6D and E) and leptomeningeal arteries are also affected (Figure 6F).

The predominant pathology—thickening of vascular walls and luminal stenosis—of arterioles, most prominent in cerebral WM and inflicting especially arterioles of smaller caliber, was explicitly demonstrated by Miao *et al* (84). This pathology is also clearly demonstrated in the elevation of the sclerotic index (SI) [defined and calculated as 1 − (internal diameter/external diameter)]. The SI of cerebral arterial vessels increased rapidly, when their lumina had narrowed to 20–30 μm and external diameter reached 130 μm. The mean SI of control persons' arterioles was about 0.42 in WM and 0.49 in GM, whereas in CADASIL patients' WM, the mean SI was 0.74 but in the relatively spared GM it increased only to 0.55 (Miao *et al* unpub. obs.). Interestingly, this increase in SI begins early, as in a 32-year-old CADASIL patient's WM arterioles the SI had reached the value of 0.64 (85). This demonstrates the remarkable difference between WM and GM arterioles, the pathobiological background of which has not yet been fully clarified. This predominant

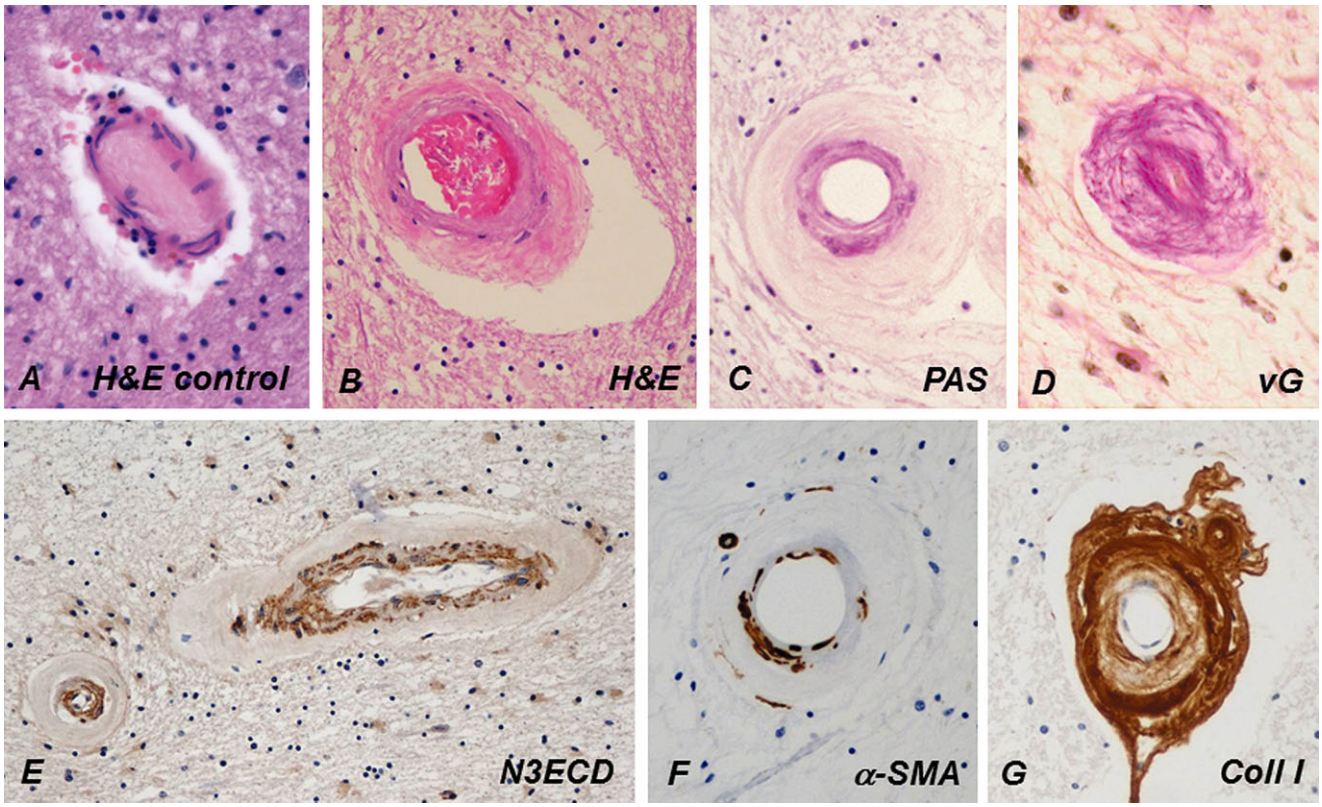

Figure 5. Compared with a control person's cerebral WM arteriole (**A**), the wall of a CADASIL patient's arteriole (**B**) is markedly thickened and fibrotic, and its rigidity renders the arteriole exceptionally circular (**C**). Tunica media is slightly basophilic in hematoxylin and eosin (H&E) (**B**) and prominently positive in periodic acid Schiff (PAS) staining (**C**). In advanced disease, the fibrosis has almost completely obliterated the lumen (**D**). Similarly, as in dermal arteries, NOTCH3 extracellular domain (N3ECD) immunopositivity accumulates in the tunica media of the thickened WM arterioles (**E**). The irregularly decreased immunoreactivity for α-smooth muscle actin (α-SMA) in the wall of a WM arteriole reflects the degeneration of VSMCs (**G**). The thickened adventitia harbors extracellular matrix proteins, here shown by collagen type I immunohistochemistry (**F**). vG = van Gieson.

stenosis in WM arterioles is also manifested in the reversal of the ratio between the mean luminal size in WM vs. cortical arterioles. In elderly controls, the mean luminal size of arterioles was found to be larger in WM than in cortex, that is 27.0 vs. 19.3 μm and the WM/GM ratio 1.40, whereas in elderly CADASIL patients, the disease had rendered the lumina of WM arterioles smaller than in cortical arterioles, that is 14.8 vs. 17.2 μm (WM/GM ratio 0.85) (Miao *et al* unpub. obs.).

The lacunar infarcts appear similar and follow the same sequence of cellular changes as any small ischemic infarct in WM, appearing at the subacute stage as a focal pannecrosis with accumulation of macrophages. For considerations on pathogenetic significance of the morphological findings, see the Pathogenetic significance of the morphological findings section.

Biopsy findings

Electron microscopy (EM) and granular osmiophilic material (GOM)

Baudrimont *et al* (7) were the first to examine a CADASIL patient's brain arteries by EM and they discovered granular electron-dense extracellular material—to be later named GOM—located in the internal part of the media, reaching the basal lamina. No amyloid or intermediate filaments were visualized and wavelength dispersive EM showed that this material was not specific for mineral or metallic elements.

The deposition of GOM has proved to be an important alteration in CADASIL. Because the arteriopathy in CADASIL is systemic, GOM deposits can be detected in arteries of many different organs, including dermal arterioles. GOMs are actually best preserved and visualized in immediately fixed skin biopsies (see Biopsy findings section; Figure 7). GOM deposits commonly have a mushroom shape with the foot closely apposed to the VSMC plasma membrane and the head projecting to the ECM. Alternatively, GOMs are irregularly rounded bodies up to 1–2 μm in diameter, usually located in indentations of VSMCs, the plasma membrane beneath being decorated by pinocytotic vesicles (Figure 7B and C insets). GOMs are also often observed in the intercellular space apparently disconnected to VSMCs (Figure 7C). GOM itself is composed of strongly osmiophilic (thus electron-dense) tiny granules Figure 7C inset).

Initial immuno-EM analysis of human brain samples showed that N3ECD accumulates at the plasma membrane of VSMCs in

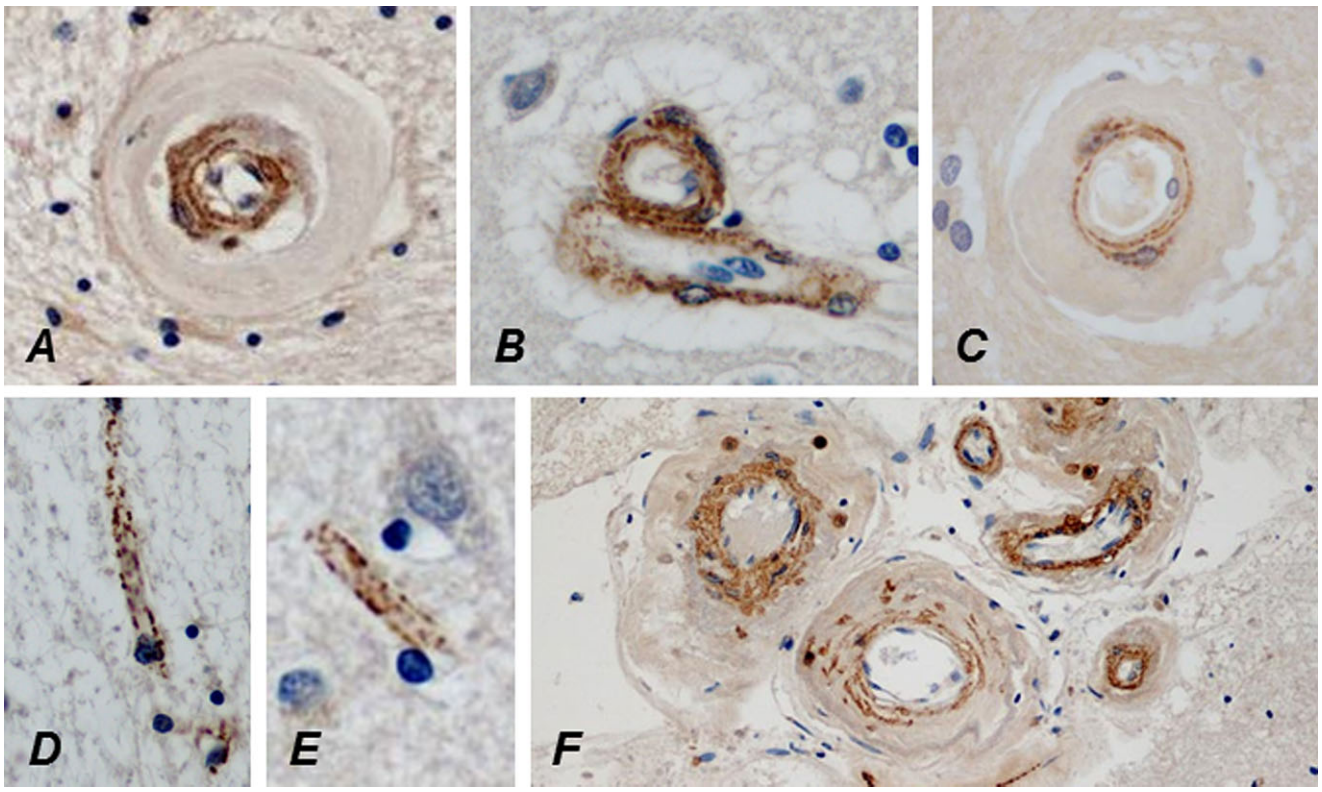

Figure 6. The lumina of a WM (**A**) and a cortical (**B**) arteriole are approximately as wide and approximately similar amount of N3ECD is deposited in their tunica media, but the wall of the WM arteriole is almost fourfold thicker than that of the cortical arteriole because of the marked fibrosis. N3ECD is also deposited in the wall of a probable vein beside the arteriole (**B**). Delicate N3ECD immunopositivity is already present in the wall of a markedly thickened arteriole in the cerebral WM of an only 32-year-old male CADASIL patient (**C**). In an elderly patient, N3ECD immunopositivity is seen on capillaries in both cerebral WM (**D**) and cortex (**E**), as well as in the walls of larger leptomeningeal arteries (**F**).

close vicinity to the GOM deposits (56). Further immunogold EM studies from our and other laboratories, using a more sensitive methodology, revealed that N3ECD is actually a component of GOM deposits (52, 91, 135). It is conceivable that the distribution of N3ECD protein is heterogeneous within the GOM deposit, and taken together the observations suggest that the concentration of N3ECD might be highest at the foot of the GOM deposit.

Because GOM has not so far been reported in any other disease, CADASIL is an exceptional form of dementia: it can be diagnosed even with a simple skin biopsy. Because its arteriopathy also involves dermal arterioles, the deposition of the above-described GOM is a specific diagnostic feature of CADASIL. In skin biopsies, GOM is detectable by EM in the walls of the diseased arterial vessels (Figure 7) as well as inconsistently of veins and rarely of capillaries. GOM appears to be present in all CADASIL patients with a pathogenic *NOTCH3* mutation that causes an uneven number of cysteines in the affected EGFr of N3ECD (122) (for details see Diagnosis of CADASIL and CARASIL section). Thus, electron microscopists consider EM analysis a highly reliable diagnostic method (92, 122). The article by Tikka *et al* (122) presents a practical approach to the EM diagnostics of CADASIL, including directions for the light microscopic selection of representative small dermal arteries for EM thin sectioning as well as interpretation of EM findings to discriminate between fallacious and true GOM deposits.

IHC of N3ECD

However, because the number of laboratories available for performing reliable EM examinations is limited, immunohistochemical demonstration of N3ECD in skin biopsy was proffered as an alternative (Figure 8) (58). It is highly sensitive (85%–95%) and specific (95%–100%), although the inherent caveats of IHC must be kept in mind. Furthermore, its applicability at an early stage of CADASIL with minimal amount of N3ECD/GOM remains to be clarified (Figure 7B). With EM, we (HK) have detected GOM in a p.Arg133Cys patient already at the age of 19 years (Figure 7B inset), and positive IHC diagnosis (AJ) was also obtained already in a 28-year-old young adult patient (58). In confocal microscopy, N3ECD immunopositivity appears as delicate dots on VSMCs (Figure 8B), in concordance with the scattered appearance of GOM deposits in EM.

As mentioned earlier a great majority of patients with unpaired cysteine in an EGFr of N3ECD appear to harbor GOM/N3ECD

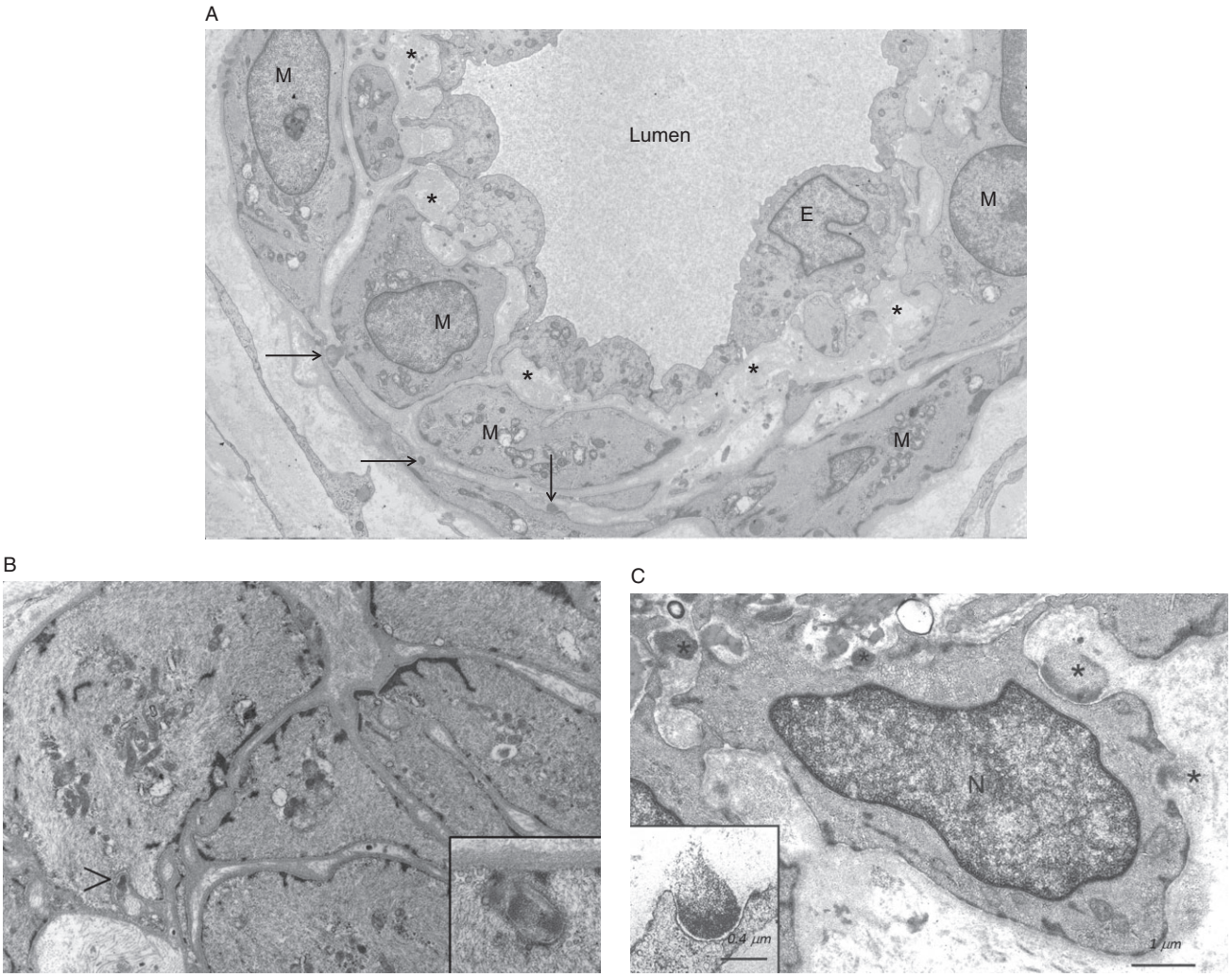

Figure 7. An electron micrograph (EM) of a small dermal artery from a 28-year-old male CADASIL patient with p.Arg133Cys NOTCH3 mutation. Three small deposits of GOM (arrows) are detectable (already at this age) on a few vascular smooth muscle cells (VSMC). The subendothelial space is widened with accumulation of extracellular matrix proteins (asterisks). E = endothelium, N = nucleus (**A**). An EM of a dermal arteriole from a 19-year-old CADASIL patient [younger brother of the patient in (A), both sons of a male patient homozygous for p.Arg133Cys mutation] shows the paucity of GOMs (arrowhead) and the inset shows that true GOMs do occur already at this young age (**B**). A higher magnification EM of a dermal arteriole from an elderly patient at a more advanced stage of the disease. GOMs are present both in indentations on a VSMC (black asterisks) and in the intercellular space apparently disconnected to the VSMC (white asterisk) (**C**). Note the pinocytotic vesicles in the VSMC beneath the GOM (**B** and **C** insets). N = nucleus. [Fig. 7A is reproduced from article (62) with permission]

deposits and therefore the presence of such a cysteine residue has been suggested to be causally associated with the formation of GOMs. However, non-cysteine mutations have been discovered in several patients with a SVD compatible with the CADASIL. Interestingly, in EM unequivocal, GOM has been reported only in two Japanese families with a non-cysteine mutation (p.Arg75Pro), in whom despite extensive search cysteine involving Notch3 mutation was not detected (87). We have not detected GOM in any of the seven non-cysteine cases that we have examined (Kalimo, unpub. obs.).

In addition to GOM deposits, EM also shows several degenerative alterations in the small arterioles: widening of subendothelial spaces, fragmentation of inner elastic lamina and presence of degenerating VSMCs with accumulation of cell debris in the extracellular space around them (122) (Figure 7A and C).

PATHOLOGY OF CARASIL

The main cerebrovascular pathology in CARASIL falls on the same vascular bed as CADASIL, that is the small penetrating arteries, mainly in the cerebral WM and basal ganglia (6, 39). Histopathologically, the arteries show advanced arteriosclerosis (Figure 9B and C) without the light microscopic basophilic granularity of tunica media or electron microscopic GOM on VSMCs as in CADASIL. Neither is there deposition of amyloid. Intima shows

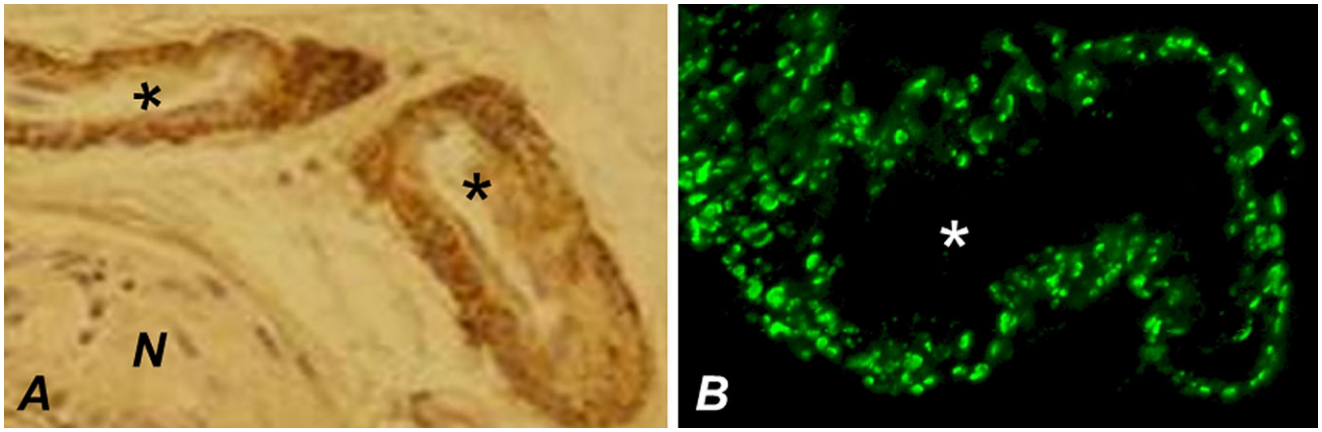

Figure 8. Immunohistochemical visualization of N3ECD deposition in the walls of dermal arteries (asterisks). The granular immunoreactivity is visualized either by using immunoperoxidase method (**A**) or—at a higher resolution—using confocal immunofluorescence, the punctate pattern being consistent with scattered distribution of GOMs (**B**). N = nerve.

fibrous thickening, internal elastic lamina is fragmented and media reveals loss of VSMCs with subsequent hyalinization. Arterial lumina are concentrically narrowed, but occasionally segmental dilation occurs. These vascular pathologies result in multifocal ischemic infarcts as well as diffuse ischemic changes, especially in cerebral WM (diffuse myelin loss with preservation of U-fibers; Figure 9A) and consequent moderate atrophy. As there is no characteristic alteration in the diseased arteries, such as GOM in CADASIL, skin biopsies do not provide any diagnostic help, neither is the systemic nature of CARASIL similarly evident as it is in CADASIL. The vascular changes in other organs affected are less severe than those in cerebral arteries.

DIAGNOSIS OF CADASIL AND CARASIL

The diagnosis of the patients, whose clinical picture is suggestive of CADASIL should be confirmed, both to inform the patient and to give correct counseling to the family members. Genetic testing is naturally the gold standard for the diagnosis of CADASIL. With the already wide knowledge of CADASIL, many genetic laboratories can provide even the full screening of the 21 (2–15, 18–24) exons that harbor the pathogenic *NOTCH3* mutations. The specificity of mutations that lead to an uneven number of cysteines within any of the 34 EGFrs in N3ECD is 100% and the sensitivity of the analysis is close to 100% (14). However, in selected cases,

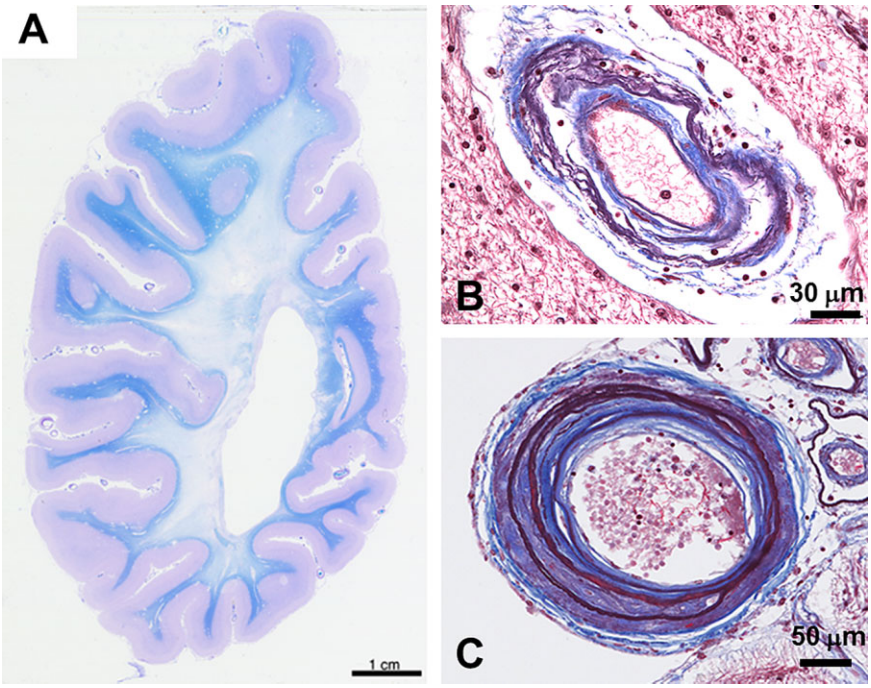

Figure 9. The cerebral white matter of a CARASIL patient who died at the age of 54 years shows diffuse widespread loss of myelin with preservation of U-fibers (**A**). A small artery from a cerebral white matter shows irregular structure with double barreling of the thickened wall. Internal elastic lamina is multiplied (**B**). The wall of a medium-sized leptomeningeal artery is markedly thickened with replacement of tunica muscularis by fibrous tissue, intimal proliferation and splitting of the internal elastic lamina. The smaller arteries beside show loose double barreling (**C**).

neuropathology can be used to ascertain the diagnosis: (i) if reliable genetic screening is not readily available or (ii) if genetic screening gives an equivocal (especially non-cysteine mutations), negative or previously unknown result (see Pathology of CADASIL section).

The clinical picture of premature alopecia, low back pain in addition to the neurological symptoms and presence of diffuse WM lesions in MRI should alert the clinician, especially in Far Eastern countries, to consider CARASIL as a possible, although a rare alternative. Similar patients among relatives indicating a hereditary disease is, of course, an important lead. The rarity of CARASIL in outside of Asia, of course, further increases the challenge in those countries. Thus, prompt molecular genetic analysis is warranted and demonstration of a pathogenic mutation in *HTRA1* gives the definite diagnosis. As mentioned earlier, skin biopsy is not an auxiliary method, although it is helpful in differential diagnosis between CARASIL and CADASIL. The differential diagnostic alternatives for CARASIL have been presented in a comprehensive reviews by Fukutake (39) and Nozaki *et al*. (97).

PATHOGENESIS

CADASIL

Although the defective gene *NOTCH3* that causes CADASIL has been identified almost 20 years ago and skilled research teams have striven to explain disease pathogenesis, the final goal has not yet been reached. The basic question whether the disease is caused by the loss-of-function or gain-of-function appears to become settled in favor of the latter alternative (see Neomorphic and toxic gain of function section).

Pathogenetic significance of the morphological findings

Vascular alterations

Stenosis of the affected arteries has been unequivocally demonstrated, but the decisive pathology—occlusion or thrombosis—of the feeding artery that leads to the lacunar infarct is rarely identified, although occasional completely obliterated arterioles may be detected (Figure 5D). In WM, where arteriolar stenosis is unequivocal, occlusion and/or thrombosis are most likely the predominant cause of the ischemic lesions. However, the arterioles with thickened and fibrotic walls, even if they are not significantly stenosed, do also bring on a risk of infarction, as demonstrated in deep GM (basal ganglia), where lacunar infarcts are common. Such arterioles have evidently lost their compliance and autoregulation, and thus the lacunar infarcts may also be caused by hemodynamic disturbances to which the rigid arterioles are not able to respond by dilatation, and critical ischemia occurs, although significant stenosis as such does not prevail (86, 119). On the other hand, experimental studies on transgenic mice expressing rat p.R169C mutant Notch3 (a preclinical mouse model of CADASIL) have shown cerebrovascular dysfunction with impaired neurovascular coupling and autoregulation of cerebral blood flow already prior to the appearance of fibrosis [and stenosis (60)]. Thus, the problem may be also functional and not only mechanistic.

In CADASIL, the blood–brain barrier (BBB) is often multifocally breached as indicated by the common appearance of multiple microbleeds in T2*w MRI [see Imaging in CADASIL section and figure 3A in (113)]. Rarely, small fresh cortical hemorrhages may be detected already during brain cutting (Figure 10A). Histopathologically, microbleeds appear as small perivascular hemosiderin or immunopositive plasma protein deposits around cortical/GM arterioles (Figure 10B and C), the walls of which are markedly thinner than in WM arterioles (Figure 10D vs. E), a likely reason for the predominant location of microbleeds in GM regions. IHC for plasma proteins shows that BBB is breached only locally at the sites of microbleeds or infarcts (Figure 10C–G), whereas the damage of the vascular walls does not appear to cause a more generalized breakdown of BBB that would result in widespread extravasation of plasma proteins and consequent vasogenic edema (Figure 10E–G). This suggests that the increased amount of free extracellular fluid detectable with DTI appears because of a CADASIL-specific type of vasogenic edema.

Tissue alterations

The interpretation of the DTI findings earlier agrees well with the analysis of the microstructural changes in transgenic mice expressing rat wt or p.Arg169Cys-mutant *Notch3* (25, 60). These mice are considered an animal model, in which the vascular and WM pathologies correspond to human preclinical CADASIL. It was demonstrated that in cerebral WM, myelin damage occurs first without loss of oligodendrocytes or major damage of axons (Figure 11). The axonal injury appears to be secondary to myelin degradation. These findings agree with the lack of an overt phenotype in these mice as well as with the fact that prominent MRI changes may be seen already in presymptomatic CADASIL patients' WM. The early WM lesions in these mice and hence in CADASIL were ascribed (linked?) to hypoperfusion-induced energy deficiency, which causes failure of ATP-dependent ion pumps and consequent impaired ion and water homeostasis. This leads to intramyelinic edema (Figure 11) (25), which in previous experimental studies has been shown to be a very early pathological change in ischemic WM (99). Chronic hypoperfusion in WM has been demonstrated both in the transgenic mouse model earlier (60) and in young CADASIL patients (127). Alternatively, impaired ion and water homeostasis could arise from a dysfunction of the astrocytic endfeet which cover the abluminal surface of pericytes and smooth muscle cells, where mutant Notch3 accumulates aberrantly (25).

Processing and trafficking of mutated Notch3

The full-length Notch3 is constitutively cleaved (site 1 = S1 cleavage) in the Golgi apparatus by furin (79) and targeted to the cell surface to form the heterodimer (N3ECD + N3TMIC, see Genetics and Biochemistry: CADASIL section and Figure 1) transmembrane receptor. It has been suggested that abnormal processing and trafficking of mutated Notch3 could be the cause of CADASIL. As almost all pathogenic mutations lead to an uneven number of cysteine residues in the mutated EGFr, the normal formation of sulphur bridges is prevented and thus misfolding of

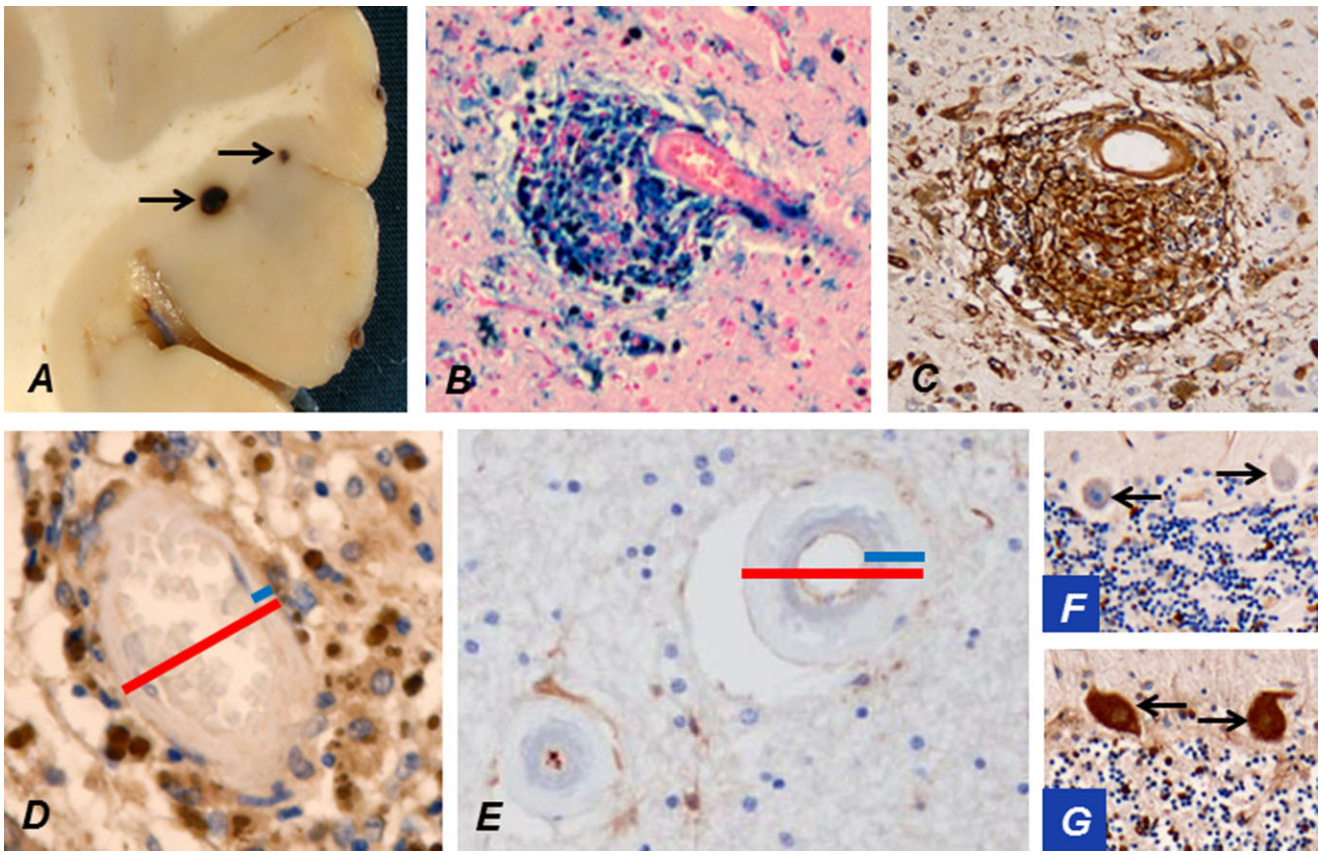

Figure 10. Occasionally microbleeds (arrows) in cerebral cortex may be visible already during brain cutting (**A**). An accumulation of hemosiderin around a cortical arteriole stains strongly positively for iron (**B**). The breached BBB at the microbleed leaks plasma fibrinogen (brown; **C**). The wall of a cortical arteriole (**D**) is markedly thinner than that of a WM arteriole (**E**; blue bars in **D** vs. **E**), while their outer diameters (red bars) are of approximately the same magnitude. This is a likely explanation for the predominant location of microbleeds in cortical and deep GM. The thick wall of a WM arteriole from a CADASIL patient at a quiescent stage of the disease has not allowed virtually any leakage of fibrinogen (**E**). Extravasated fibrinogen is normally taken up by Purkinje cells (PCs) from cerebrospinal fluid (51). Thus, negative fibrinogen staining of cerebellar PCs (arrows; **F**) verifies that significant leakage has not occurred in this patient at a quiescent stage, whereas in another CADASIL patient, who had suffered an infarct just before death, PCs (arrows) are strongly immunopositive for fibrinogen reflecting the breakdown of BBB (**G**).

Notch3 most likely occurs. However, misfolded Notch3 proteins appear to escape the normal cellular quality control, ubiquitylation and proteosomal degradation, and are correctly processed and transported to cell surface in their partially misfolded state.

For example, in genuine patient-derived VSMCs (with p.R133C mutation) cultured *in vitro*, the S1 cleavage appeared to occur correctly and intracellular aggregates were not more frequent than in control VSMCs. This suggests that in human VSMCs the microenvironment in Golgi and ER is able to prevent intracellular interreceptor cross-linking and aggregation of the mutated endogenous Notch3 (123). Thus, the characteristic aggregation of N3ECD does not appear to occur until the receptor has reached the cell surface and therefore the accumulation of N3ECD on VSMCs is most likely because of its local aggregation and/or its impaired clearance (34, 91).

In experimental studies, normal intracellular processing, trafficking and signaling were reported by Joutel *et al* (59) in cells transfected with human *NOTCH3* harboring three different mutations and by Low *et al* (80) with *NOTCH3* harboring four different mutations. However, in a study by Peters *et al* (100), cells transfected with mutated human *NOTCH3* (p.R133C, p.C183R and p.C455R) showed reduced S1 (furin) cleavage. In another study, in cells transfected with mutated mouse mNotch3, a lesser amount of the overexpressed mutated than wt mNotch3 was transported to the cell surface. Besides, intracellular aggregates were formed, which may have resulted from increased accumulation or slowed transport in the secretory pathway (63). Abnormal S1 cleavage was also reported in cells expressing mutated rat Notch3, but presentation of this Notch3 on the cell surface was preserved (46). Yet, in the latter three studies, signaling by these mutated Notch3 receptors was not compromised. Thus, defective proteolytic processing or intracellular trafficking does not appear to be the key problem in CADASIL.

Impaired Notch3 signaling

Although many of the studies earlier have shown that mutated Notch3 retains its canonical signaling, loss of function has not

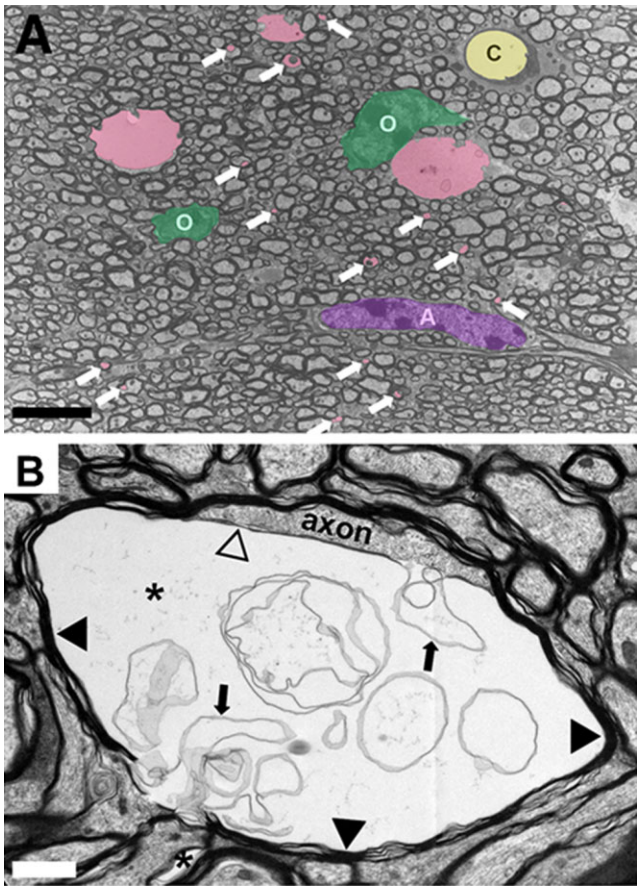

Figure 11. (**A**) Representative electron micrographs of the corpus callosum from a TgPAC-Notch3^{R169C} showing multiple membrane-bound vacuoles (colored in pink) including numerous inframicrometric vacuoles (white arrows). O = oligodendrocytes (colored in green); A = astrocyte (colored in purple); C = capillary (colored in yellow). (**B**) Typical large vacuole (asterisk) in the innermost layer of the myelin sheath. The vacuole separates the axon from its myelin sheath (black arrowheads) and contains multiple aberrant myelin sheets (arrows). Notice the thin myelin sheet (open arrowhead) at the interface between the axon and the vacuole. *Scale bar* represents 5 μm in (A) and 1 μm in (B).

been fully abandoned as a possible pathogenetic mechanism. Hypomorphic Notch3 function was suggested by Arboleda-Velasquez *et al* (5) to be associated with CADASIL pathophysiology. They applied an *in vivo* assay, with which they showed that mutated (p.Cys455Arg or p.Arg1031Cys) *NOTCH*3 transgenes did not rescue the ischemic susceptibility phenotype of *Notch3* knockout mice (evaluated by measuring the infarct size after standard filament occlusion of middle cerebral artery) as efficiently as wt *NOTCH3*. They also demonstrated decreased signaling activity in embryonic fibroblasts from transgenic mice expressing the above-mentioned mutated *NOTCH3* genes co-cultured with ligand Delta-like 1 expressing cells.

However, in some patients, CADASIL is caused by mutations at the ligand binding site, which abrogate ligand binding to Notch3 (Figure 1). Yet, the clinical pictures of these patients and of those with mutations outside the binding site are very similar. Thus, it is somewhat difficult to accept that the loss of function would be the sole/main cause of CADASIL. This view is supported for example by the experiments of Joutel *et al* (59) and Peters *et al* (100), who demonstrated *in vitro* that only Notch3 with specific mutations located in the ligand binding site in EGF repeats 10–11 (p.Cys428Ser and p.Cys455Arg) exhibited significantly reduced transcriptional activity via the RBP-Jκ pathway, whereas the tested Notch3 receptors with mutations located outside the binding site had nearly normal signaling activity. In another set of *in vivo* experiments, the physiological levels of both wt human NOTCH3 and mutant p.Arg90Cys human NOTCH3 rescued the arterial defects of Notch3 knockout mice to similar degrees and mutant *Notch3* exhibited normal level of Notch3/RBP-Jκ activity in brain arteries (89). Furthermore, *Notch3*-deficient (knockout) mice do not develop CADASIL pathognomonic GOM deposits or CADASIL pathology (23, 24, 65, 67), whereas they do appear in transgenic mice expressing mutant *Notch3* (5, 89, 111), but these deposits do not interfere with Notch3/RBP-Jκ signaling activity (23, 24, 89). Finally, elimination of wt *Notch3* did not influence the onset and burden of WM lesions in the TgPAC-*Notch3*^{R169C} mice (23). Besides, the similar phenotype in the homozygous and heterozygous CADASIL patients (126) as well as the lack of truncating mutations in CADASIL (100) also favor a mechanism other than loss of the canonical Notch3 function.

Neomorphic and toxic gain of function

Thus, majority of CADASIL studies seem to favor a neomorphic (gain of novel function) pathogenetic mechanism rather than compromised canonical Notch3 function. The alteration that is common to all CADASIL mutations is the accumulation of N3ECD on the VSMC surface; unpaired cysteine residue with consequent partial misfolding and/or abnormal glycosylation of Notch3 seem to cause aberrant dimerization and higher order multimerization with cross-linking by disulphide bonds, which results in the aggregation and deposition of N3ECD on VSMC surface (5, 34, 91). This aggregation phenomenon was also demonstrated in several transgenic mice expressing mutated (p.Arg90Cys or p.Cys428Ser) human Notch3 or (p.Arg169Cys) rat Notch3 and in a knocked-in mouse model expressing the corresponding mouse p.Arg169Cys mutation, which did accumulate N3ECD on VSMCs like in CADASIL patients (23, 24, 89, 90, 111). Normally, N3ECD is transendocytosed into the ligand-expressing cell and degraded through the endocytic-lysosomal degradation pathway (44). The observation of abnormal accumulation of N3ECD in the vascular wall without accumulation of N3TMIC has raised the possibility that upon ligand binding, mutant Notch3 might be refractory to transendocytosis and further degradation (134). However, against this possibility speaks the observation that both transgenic mice and patients carrying the p.Cys428Ser mutation, which abolishes binding of the DSL ligands to Notch3, harbor vascular N3ECD deposits (59, 90). How mutated N3ECD may cause degeneration of VSMCs and the other con/subsequent pathogenic alterations has remained enigmatic.

Most studies have shown that neither most mutations in Notch3 nor accumulation of N3ECD compromise the canonical signaling, yet this accumulation appears to be pathogenic. The retention of misfolded N3ECD with an unpaired cysteine, could result in novel protein–protein interactions and induce (inactivate or aggravate)

still unknown functions/dysfunctions that are toxic to VSMCs. A recent study showed that N3ECD deposits can make up a platform or act as a seed that promotes interactions with ECM proteins, such as tissue inhibitor of metalloproteinases 3 (TIMP3), that in turn can bind and recruit more and more proteins, such as vitronectin, generating new interaction surfaces and magnifying the toxic potential of aggregates in a snowball effect (91). Abnormal sequestration of proteins into aggregates usually results in the collapse of their biological function (98). TIMP3 and vitronectin have multiple biological activities that are directly relevant to CADASIL pathogenesis. For example, TIMP3 dysregulation could contribute to small vessel pathology through its well-known metalloproteinase inhibitory activity. Also, by its ability to bind and stabilize plasminogen activator inhibitor-1, vitronectin could modulate the balance of the fibrinolytic system, and consequently, the ECM homeostasis. Further studies are required to examine whether and how focal TIMP3 and vitronectin deposition can alter their biological activities and contribute to the disease process. Intriguingly, our preliminary studies showed an unexpected elevation of TIMP3 activity in the brain vessels of both CADASIL mouse models and patients with CADASIL.

A definite response is the degeneration of VSMCs with consequent impairment of vasomotor functions. This is reflected in the pathology of the key smooth muscle cell contractile protein α-actin (interestingly, α-actin is a direct target of canonical Notch3 signaling, yet disturbance in this pathway was by and large excluded). In cultured genuine human CADASIL (p.Arg133Cys) VSMCs, several proteins interacting with actin cytoskeleton were differentially expressed and the contractile capability of these VSMCs was impaired (50). In these cells, the actin cytoskeleton showed many derangements, the severity of which varied in VSMCs from different vascular beds being most severe in VSMCs derived from adult cerebral arteries. Again in slight disagreement with the above-described lesser pathogenicity of hypomorphic Notch signaling, short hairpin RNA (shRNA) silencing of *NOTCH3* in control cells did cause similar derangements of actin as in the p.Arg133Cys mutant human VSMCs (123). Furthermore, these cells disclosed also other features of hypomorphic Notch3 signaling by showing reduced upregulation of expression of Notch3 target genes *PDGFR*-β, *HES1* and *HEY1* in response to ligand activation (53).

Degeneration of VSMCs is followed by increased production of ECM proteins resulting in marked thickening of the arterial walls, stenosis and decreased compliance [see above Pathology of CADASIL section and (84)]. Whether this is a general response to degeneration of VSMCs or because of the activation of Notch-specific fibrotic pathways is still to be examined (see discussion on TGF-β signaling in CARASIL). By IHC, it has been shown that in CADASIL types I, II, IV and VI collagens are consistently increased in the walls of all caliber arterial vessels (31). These findings agree well with those in the study by Monet-Leprêtre *et al* (91) in which the activity of TIMP3 was significantly elevated in both human patients and transgenic mouse model of CADASIL, as such an anticipated finding in vessel fibrosis reflecting reduced degradation of ECM components. Whether fibrosis also reflects transformation of VSMCs from contractile to productive mode like in atherosclerosis (68) is not known, although because VSMCs are degenerating, the most likely cell to produce ECM proteins is fibroblast.

CARASIL

Contrary to the complicated pathogenesis in CADASIL, the pathogenetic mechanisms in CARASIL appear relatively straightforward (45, 97, 116). As described in more detail in the section Genetics and Biochemistry, the function of HTRA1 as a repressor of TGF-β signaling by cleaving proTGF-β1 in the ER results in reduced amounts of mature TGF-β1 in the ECM. HTRA1 mutations have been demonstrated to result in its decreased function and consequently in greater amounts of mature TGF-β and upregulation of TGF-β signaling. TGF-β plays a critical role in ECM accumulation and vascular remodeling via upregulating the production of several agents including connective tissue growth factor (CTGF) and fibroblast growth factor. It has been shown to be the key mediator of vascular fibrosis (71). Concordantly, with the skeletal pathologies in CARASIL, TGF-β also uniquely coordinates bone cell activity to maintain bone homeostasis. It regulates the differentiation and function of both osteoblasts and osteoclasts, from lineage recruitment to terminal differentiation, thereby balancing bone formation and resorption (121).

THERAPEUTIC ASPECTS

CADASIL

Because CADASIL is an autosomal dominant genetic disease, preventing the expression of the mutated pathogenic allele of *NOTCH3* should—if successful—provide definite therapy. Based on the assumption that the decisive pathogenesis is the toxic gain of function, probably associated with the unpaired cysteine in the affected EGFr/EGFrs, there are two possible gene therapeutic approaches: (i) silencing the mutated gene allele with inhibitory RNA molecules and (ii) antisense-mediated skipping of the *NOTCH3* exon harboring the defective DNA sequence. Allele-specific siRNAs have already been designed for several diseases, including familial forms of Alzheimer's disease, Parkinson's disease, amyotrophic lateral sclerosis and spinocerebellar ataxia 7 (66, 114). Tikka *et al* (123) demonstrated efficient silencing of *NOTCH3* in control VSMCs (from human umbilical artery) transfected with two different vectors (by 36% respectively 63%), which encode shRNAs targeting *NOTCH3* gene. This predicts that the expression of the mutated *NOTCH3* could also be silenced and thereby the assumed toxic effect could be prevented. Because of the great number of pathogenic mutations this approach would require a production of very many vectors to specifically silence only the pathogenic allele. A more inclusive possibility would be antisense-mediated exon skipping, which is emerging as a promising gene therapy to combat Duchenne muscular dystrophy, a hereditary disease with a markedly larger number of different mutations than in CADASIL (1, 49). This approach would be advantageous also in CADASIL, because skipping of a few exons, for example exons 3 and 4 encoding EGFr 2–5, which harbor a large cluster of missense mutations [>40% of mutations in >70% of families occur in these exons (18)], could—if successful—produce a truncated Notch3 in which the unpaired cysteine is eliminated, but at the same time it should still remain capable of implementing Notch3 functions. Thus, a limited number of skipping procedures could help many patients. The location of VSMCs

just beyond the endothelium from circulating blood may well facilitate delivery of the antisense oligonucleotides to the target cell, VSMC.

Despite the promising gene therapeutic views, at present, only symptomatic therapy is available, beginning with the simple recommendation to refrain from smoking. If the migraneous headache requires medication, conventional "pain killers" are recommended, whereas treatment with classic migraine drugs, such as ergotamines or triptans is discouraged because of their vasoconstrictory effect (13). Exceptionally, acetazolamide has been applied to alleviate acute excruciating migraine attacks (36).

Anticoagulants and antiaggregants have been tried without definite positive effects; rather these medications may have caused a few fatal parenchymal brain hemorrhages. As the progressive stenosis and rigidity already impair blood flow in the diseased arterioles, increased blood viscosity, for example because of polycythemia or dehydration, appears to be harmful and should be avoided (Viitanen, unpub. obs.). On the same basis, medications which cause cerebral hypoperfusion, such as antihypertensive drugs, tricyclic antidepressants and neuroleptics, should be administered with caution. Because one-half of the CADASIL patients have hypercholesterolemia, treatment with statins is indicated, although the role of statins in CADASIL *per se* is still unknown (102).

Cognitive decline begins already before ischemic attacks. Cholinergic deficits have been found in CADASIL patients in late middle age (64) and therefore cholinesterase inhibitors may alleviate cognitive decline. In a placebo controlled study with donepezil, executive functions were improved moderately but the clinical relevance of this treatment is still unknown (30).

CARASIL

For CARASIL, there is at present no effective treatment (39). The genetic defect causes a loss-of-function of HTRA1, which would necessitate inducing production of functional HTRA1 (or administration of another molecule capable of repressing TGF-β signaling). Thus, similar approaches as suggested earlier for CADASIL, in which the toxic gain-of-function now seems to be the plausible pathogenic mechanism, are not possible. Shiga *et al* (116) and Nozaki *et al*. (97) proposed interesting approaches to treat patients carrying a nonsense mutation of *HTRA1*. Preventing/alleviating the nonsense-mediated decay of mutated mRNA might be effective in increasing truncated p.Arg370X HTRA1, which has been shown to retain normal protease activity, since the truncated C-terminal PDZ domain of HTRA1 was revealed to be dispensable (18, 97, 117). Alternatively a drug (e.g. aminoglycoside antibiotics) that suppresses the identification of the translation termination codon (induced by the mutation), may allow, sufficient production of active HTRA1 and thus repression of TGF-β signaling could be rescued.

The treatment at present includes prevention of non-CARASIL-related ischemic stroke, genetic counseling, supportive care and medications for treating dementia. The roles of antithrombotic and anticoagulant drugs in the therapeutics are still unclear (39).

Because excessive TGF-β signaling appears to be the major culprit in CARASIL, another approach—direct inhibition of TGF-β signaling—has been suggested to be investigated as a therapeutic strategy (97). This suggestion is based on the fact that in Marfan syndrome, which is also caused by increased TGF-β signaling, angiotensin I receptor antagonist (a drug in clinical use as antihypertensive) has been shown to inhibit TGF-β signaling and ameliorate the progression of Marfan syndrome in both transgenic mice and patients. In human brain, angiotensin I receptor antagonist also inhibits TGF-β signaling (97).

ACKNOWLEDGMENTS

This study was supported by EVO research funds of the Helsinki University Hospital to the Finnish CADASIL team, Sigrid Juselius Foundation and Maud Kuistila Foundation, Finland to S.T., Fondation Leducq (Transatlantic Network of Excellence on the Pathogenesis of Small Vessel Disease of the Brain), France to A.J., Finnish Cultural Foundation, Varsinais-Suomi regional fund, Finland to M.S. And we thank Prof. Osamu Onodera, Niigata University, Japan for the genetic analyses and Dr Shigeo Murayama, Departments of Neurology and Neuropathology, Tokyo Metropolitan Geriatric Hospital and Institute of Gerontology, Japan for the neuropathological examinations on CARASIL.

REFERENCES

1. Aartsma-Rus A, Fokkema I, Verschuuren J, Ginjaar I, van Deutekom J, van Ommen GJ, den Dunnen JT (2009) Theoretic applicability of antisense-mediated exon skipping for Duchenne muscular dystrophy mutations. *Hum Mutat* **30**:293–299.
2. Adib-Samii P, Brice G, Martin RJ, Markus HS (2010) Clinical spectrum of CADASIL and the effect of cardiovascular risk factors on phenotype. Study in 200 consecutively recruited individuals. *Stroke* **41**:630–634.
3. Amberla K, Wäljas M, Tuominen S, Almqvist O, Pöyhönen M, Tuisku S *et al* (2004) Insidious cognitive decline in CADASIL. *Stroke* **35**:1598–1602.
4. Arboleda-Velasquez J, Rampal R, Fung E, Darland DC, Liu M, Martinez MC *et al* (2005) CADASIL mutations impair Notch3 glycosylation by Fringe. *Hum Mol Genet* **14**:1631–1649.
5. Arboleda-Velasquez JF, Manent J, Lee JH, Tikka S, Ospina C, Vanderburg CR *et al* (2011) Hypomorphic Notch3 alleles link Notch signaling to ischemic cerebral small-vessel disease. *Proc Natl Acad Sci U S A* **108**:E128–E135.
6. Arima K, Yanagawa S, Ito N, Ikeda S (2003) Cerebral arterial pathology of CADASIL and CARASIL (Maeda syndrome). *Neuropathology* **23**:327–334.
7. Baudrimont M, Dubas F, Joutel A, Tournier-Lasserve E, Bousser MG (1993) Autosomal dominant leukoencephalopathy and subcortical ischemic stroke. A clinicopathological study. *Stroke* **24**:122–125.
8. Bayrakli F, Balaban H, Gurelik M, Hizmetli S, Topaktas S (2014) Mutation in the HTRA1 gene in a patient with degenerated spine as a component of CARASIL syndrome. *Turk Neurosurg* **24**:67–69.
9. Bianchi S, Di Palma C, Gallus GN, Taglia I, Poggiani A, Rosini F *et al* (2014) Two novel HTRA1 mutations in a European CARASIL patient. *Neurology* **82**:898–900.
10. Bouvy WH, Biessels GJ, Kuijf HJ, Kappelle LJ, Luijten PR, Zwanenburg JJ (2014) Visualization of perivascular spaces and perforating arteries with **7** T magnetic resonance imaging. *Invest Radiol* **49**:307–313.
11. Bozkulak EC, Weinmaster G (2009) Selective use of ADAM10 and ADAM17 in activation of Notch1 signaling. *Mol Cell Biol* **29**:5679–5695.

12. Bruening R, Dichgans M, Berchtenbreiter C, Yousry T, Seelos KC, Wu RH *et al* (2001) Cerebral autosomal dominant arteriopathy with subcortical infarcts and leukoencephalopathy: decrease in regional cerebral blood volume in hyperintense subcortical lesions inversely correlates with disability and cognitive performance. *AJNR Am J Neuroradiol* **22**:1268–1274.
13. Chabriat H, Bousser MG (2008) Cerebral autosomal dominant arteriopathy with subcortical infarcts and leukoencephalopathy. *Handb Clin Neurol* **89**:671–686.
14. Chabriat H, Vahedi K, Iba-Zizen MT, Joutel A, Nibbio A, Nagy TG *et al* (1995a) Clinical spectrum of CADASIL: a study of 7 families. Cerebral autosomal dominant arteriopathy with subcortical infarcts and leukoencephalopathy. *Lancet* **346**:934–939.
15. Chabriat H, Bousser M-G, Pappata S (1995b) Cerebral autosomal dominant arteriopathy with subcortical infarcts and leukoencephalopathy: a positron emission tomography study in two affected family members. *Stroke* **26**:1729–1730.
16. Chabriat H, Pappata S, Poupon C, Clark CA, Vahedi K, Poupon F *et al* (1999) Clinical severity in CADASIL related to ultrastructural damage in white matter: in vivo study with diffusion tensor MRI. *Stroke* **30**:2637–2643.
17. Chabriat H, Pappata S, Ostergaard L, Clark CA, Pachot-Clouard M, Vahedi K *et al* (2000) Cerebral hemodynamics in CADASIL before and after acetazolamide challenge assessed with MRI bolus tracking. *Stroke* **31**:1904–1912.
18. Chabriat H, Joutel A, Dichgans M, Tournier-Lasserve E, Bousser MG (2009) CADASIL. *Lancet Neurol* **8**:643–653.
19. Chen Y, He Z, Meng S, Li L, Yang H, Zhang X (2013) A novel mutation of the high-temperature requirement A serine peptidase 1 (HTRA1) gene in a Chinese family with cerebral autosomal recessive arteriopathy with subcortical infarcts and leukoencephalopathy (CARASIL). *J Int Med Res* **41**:1445–1455.
20. Choi EJ, Choi CG, Kim JS (2005) Medium to large cerebral artery involvement in CADASIL. *Neurology* **65**:1322–1324.
21. Choi JC, Lee KH, Song SK, Lee JS, Kang SY, Kang JH (2013a) Screening for *NOTCH3* gene mutations among 151 consecutive Korean patients with acute ischemic stroke. *J Stroke Cerebrovasc Dis* **22**:608–614.
22. Choi JC, Song SK, Lee JS, Kang SY, Kang JH (2013b) Diversity of stroke presentation in CADASIL: study from patients harboring the predominant Notch3 mutation R544C. *J Stroke Cerebrovasc Dis* **22**:126–131.
23. Cognat E, Hervé D, Joutel A (2014a) Response to letter regarding article, "Archetypal Arg169Cys mutation in Notch3 does not drive the pathogenesis in cerebral autosomal dominant arteriopathy with subcortical infarcts and leucoencephalopathy via a loss-of-function mechanism". *Stroke* **45**:e129.
24. Cognat E, Baron-Menguy C, Domenga-Denier V, Cleophax S, Fouillade C, Monet-Leprêtre M *et al* (2014b) Archetypal Arg169Cys mutation in Notch3 does not drive the pathogenesis in cerebral autosomal dominant arteriopathy with subcortical infarcts and leucoencephalopathy via a loss-of-function mechanism. *Stroke* **45**:842–849.
25. Cognat E, Cleophax S, Domenga-Denier V, Joutel A (2014c) Early white matter changes in CADASIL: evidence of segmental intramyelinic oedema in a pre-clinical mouse model. *Acta Neuropathol Commun*. **2**:49. doi: 10.1186/2051-5960-2-49
26. Cumurciuc R, Henry P, Gobron C, Vicaut E, Bousser MG, Chabriat H, Vahedi K (2006) Electrocardiogram in cerebral autosomal dominant arteriopathy with subcortical infarcts and leukoencephalopathy patients without any clinical evidence of coronary artery disease: a case-control study. *Stroke* **37**:1100–1102.
27. Dichgans M (2009) Cognition in CADASIL. *Stroke* **40**:S45–S47.
28. Dichgans M, Mayer M, Uttner I *et al* (1998) The phenotypic spectrum of CADASIL: clinical findings in 102 cases. *Ann Neurol* **44**:731–739.
29. Dichgans M, Holtmannspotter M, Herzog J, Peters N, Bergmann M, Yousry TA (2002) Cerebral microbleeds in CADASIL: a gradient-echo magnetic resonance imaging and autopsy study. *Stroke* **33**:67–71.
30. Dichgans M, Markus HS, Salloway S, Verkkoniemi A, Moline M, Wang Q *et al* (2008) Donepezil in patients with subcortical vascular cognitive impairment: a randomised double-blind trial in CADASIL. *Lancet Neurol* **7**:310–318.
31. Dong H, Blaivas M, Wang MM (2012) Bidirectional encroachment of collagen into the tunica media in cerebral autosomal dominant arteriopathy with subcortical infarcts and leukoencephalopathy. *Brain Res* **1456**:64–71.
32. Dong Y, Hassan A, Zhang Z, Huber D, Dalageorgou C, Markus HS (2003) Yield of screening for CADASIL mutations in lacunar stroke and leukoaraiosis. *Stroke* **34**:203–205.
33. Dubroca C, Lacombe P, Domenga V, Maciazek J, Levy B, Tournier-Lasserve E *et al* (2005) Impaired vascular mechanotransduction in a transgenic mouse model of CADASIL arteriopathy. *Stroke* **36**:113–117.
34. Duering M, Karpinska A, Rosner S, Hopfner F, Zechmeister M, Peters N *et al* (2011) Co-aggregate formation of CADASIL-mutant Notch3: a single-particle analysis. *Hum Mol Genet* **20**:3256–3265.
35. Fleming RJ, Hori K, Sen A, Filloramo GV, Langer JM, Obar RA *et al* (2013) An extracellular region of Serrate is essential for ligand-induced cis-inhibition of Notch signaling. *Development* **140**:2039–2049.
36. Forteza AM, Brozman B, Rabinstein AA, Romano JG, Bradley WG (2001) Acetazolamide for the treatment of migraine with aura in CADASIL. *Neurology* **57**:2144–2145.
37. Fouillade C, Monet-Leprêtre M, Baron-Menguy C, Joutel A (2012) Notch signalling in smooth muscle cells during development and disease. *Cardiovasc Res* **95**:138–146.
38. Fouillade C, Baron-Menguy C, Domenga-Denier V, Thibault C, Takamiya K, Huganir R, Joutel A (2013) Transcriptome analysis for Notch3 target genes identifies Grip2 as a novel regulator of myogenic response in the cerebrovasculature. *Arterioscler Thromb Vasc Biol* **33**:76–86.
39. Fukutake T (2011) Cerebral autosomal recessive arteriopathy with subcortical infarcts and leukoencephalopathy (CARASIL): from discovery to gene identification. *J Stroke Cerebrovasc Dis* **20**:85–93.
40. Fukutake T, Hirayama K (1995) Familial young adult–onset arteriosclerotic leukoencephalopathy with alopecia and lumbago without arterial hypertension. *Eur Neurol* **35**:69–79.
41. Gobron C, Viswanathan A, Bousser MG, Chabriat H (2006) Multiple simultaneous cerebral infarctions in cerebral autosomal dominant arteriopathy with subcortical infarcts and leukoencephalopathy. *Cerebrovasc Dis* **22**:445–446.
42. Gobron C, Vahedi K, Vicaut E, Stucker O, Laemmel E, Baudry N *et al* (2007) Characteristic features of *in vivo* skin microvascular reactivity in CADASIL. *J Cereb Blood Flow Metab* **27**:250–257.
43. Granild-Jensen J, Jensen UB, Schwartz M, Hansen US (2009) Cerebral autosomal dominant arteriopathy with subcortical infarcts and leukoencephalopathy resulting in stroke in an 11-year-old male. *Dev Med Child Neurol* **51**:754–757.
44. Hansson EM, Lanner F, Das D, Mutvei A, Marklund U, Ericson J *et al* (2010) Control of Notch-ligand endocytosis by ligand-receptor interaction. *J Cell Sci* **123**:2931–2942.

45. Hara K, Shiga A, Fukutake T, Nozaki H, Miyashita A, Yokoseki A *et al* (2009) Association of HTRA1 mutations and familial ischemic cerebral small-vessel disease. *N Engl J Med* **360**:1729–1739.
46. Haritunians T, Chow T, De Lange RP, Nichols JT, Ghavimi D, Dorrani N *et al* (2005) Functional analysis of a recurrent missense mutation in Notch3 in CADASIL. *J Neurol Neurosurg Psychiatry* **76**:1242–1248.
47. Harju M, Tuominen S, Summanen P, Viitanen M, Pöyhönen M, Nikoskelainen E *et al* (2004) Scanning laser Doppler flowmetry shows reduced retinal capillary blood flow in CADASIL. *Stroke* **35**:2449–2452.
48. Hartley J, Westmacott R, Decker J, Shroff M, Yoon G (2010) Childhood-onset CADASIL: clinical, imaging, and neurocognitive features. *J Child Neurol* **25**:623–627.
49. Hoffman EP, McNally EM (2014) Exon-skipping therapy: a roadblock, detour, or bump in the road? *Sci Transl Med*. **6**(230):230fs14. doi: 10.1126/scitranslmed.3008873
50. Ihalainen S, Soliymani R, Iivanainen E, Mykkänen K, Sainio A, Pöyhönen M *et al* (2007) Proteome analysis of cultivated vascular smooth muscle cells from a CADASIL patient. *Mol Med* **13**:305–314.
51. Ikegaya H, Heino J, Laaksonen H, Toivonen S, Kalimo H, Saukko P (2004) Accumulation of plasma proteins in Purkinje cells as an indicator of blood-brain barrier breakdown. *Forensic Sci Int* **146**:121–124.
52. Ishiko A, Shimizu A, Nagata E, Takahashi K, Tabira T, Suzuki N (2006) Notch3 ectodomain is a major component of granular osmiophilic material (GOM) in CADASIL. *Acta Neuropathol* **112**:333–339.
53. Jin S, Hansson EM, Tikka S, Lanner F, Sahlgren C, Farnebo F *et al* (2008) Notch signaling regulates platelet-derived growth factor receptor-beta expression in vascular smooth muscle cells. *Circ Res* **102**:1483–1491.
54. Joutel A, Corpechot C, Ducros A, Vahedi K, Chabriat H, Mouton P *et al* (1996) Notch3 mutations in CADASIL, a hereditary late-onset condition causing ischaemic stroke and dementia. *Nature* **383**:707–710.
55. Joutel A, Dodick DD, Parisi JE, Cecillon M, Tournier-Lasserve E, Bousser MG (2000a) De novo mutation in the *NOTCH3* gene causing CADASIL. *Ann Neurol* **47**:388–391.
56. Joutel A, Andreux F, Gaulis S, Domenga V, Cecillon M, Battail N *et al* (2000b) The ectodomain of the Notch3 receptor accumulates within the cerebrovasculature of CADASIL patients. *J Clin Invest* **105**:597–605.
57. Joutel A, Chabriat H, Vahedi K, Domenga V, Vayssière C, Ruchoux MM *et al* (2000c) Splice site mutation causing a seven amino acid Notch3 in-frame deletion in CADASIL. *Neurology* **54**:1874–1875.
58. Joutel A, Favrole P, Labauge P, Chabriat H, Lescoat C, Andreux F *et al* (2001) Skin biopsy immunostaining with a Notch3 monoclonal antibody for CADASIL diagnosis. *Lancet* **358**:2049–2051.
59. Joutel A, Monet M, Domenga V, Riant F, Tournier-Lasserve E (2004) Pathogenic mutations associated with cerebral autosomal dominant arteriopathy with subcortical infarcts and leukoencephalopathy differently affect Jagged1 binding and Notch3 activity via the RBP/Jκ signaling pathway. *Am J Hum Genet* **74**:338–347.
60. Joutel A, Monet-Leprêtre M, Gosele C, Baron-Menguy C, Hammes A, Schmidt S *et al* (2010) Cerebrovascular dysfunction and microcirculation rarefaction precede white matter lesions in a mouse genetic model of cerebral ischemic small vessel disease. *J Clin Invest* **120**:433–445.
61. Kalimo H, Ruchoux MM, Viitanen M, Kalaria RN (2002) CADASIL a common form of hereditary arteriopathy causing brain infarcts and dementia. *Brain Pathol* **12**:371–384.
62. Kalimo H, Miao Q, Tikka S, Mykkänen K, Junna M, Roine S *et al* (2008) CADASIL, the most common hereditary vascular subcortical dementia. *Future Neurol* **3**:683–704.
63. Karlström H, Beatus P, Dennaeus K, Chapman G, Lendahl U, Lundqvist J (2002) A CADASIL mutated receptor exhibits impaired intracellular trafficking and maturation but normal ligand-induced signaling. *Proc Natl Acad Sci U S A* **99**:17119–17124.
64. Keverne JS, Low WC, Ziabreva I, Court JA, Oakley AE, Kalaria RN (2007) Cholinergic neuronal deficits in CADASIL. *Stroke* **38**:188–191.
65. Kitamoto T, Takahashi K, Takimoto H, Tomizuka K, Hayasaka M, Tabira T, Hanaoka K (2005) Functional redundancy of the Notch gene family during mouse embryogenesis: analysis of Notch gene expression in Notch3-deficient mice. *Biochem Biophys Res Commun* **331**:1154–1162.
66. Koutsilieri E, Rethwilm A, Scheller C (2007) The therapeutic potential of siRNA in gene therapy of neurodegenerative disorders. *J Neural Transm Suppl* **72**:43–49.
67. Krebs LT, Xue Y, Norton CR, Sundberg JP, Beatus P, Lendahl U *et al* (2003) Characterization of Notch3-deficient mice: normal embryonic development and absence of genetic interactions with Notch 1 mutation. *Genesis* **37**:139–143.
68. Lacolley P, Regnault V, Nicoletti A, Li Z, Michel JB (2012) The vascular smooth muscle cell in arterial pathology: a cell that can take on multiple roles. *Cardiovasc Res* **95**:194–204.
69. Lacombe P, Oligo C, Domenga V, Tournier-Lasserve E, Joutel A (2005) Impaired cerebral vasoreactivity in a transgenic mouse model of cerebral autosomal dominant arteriopathy with subcortical infarcts and leukoencephalopathy arteriopathy. *Stroke* **36**:1053–1058.
70. Laitinen V, Siitonen M, Pasanen P (2008) Previously unpublished data. DNA Diagnostic Laboratory, Department of Medical Genetics, University of Turku, Turku, Finland.
71. Lan TH, Huang XQ, Tan HM (2013) Vascular fibrosis in atherosclerosis. *Cardiovasc Pathol* **22**:401–407.
72. Lee YC, Liu CS, Chang MH, Lin KP, Fuh JL, Lu YC *et al* (2009) Population-specific spectrum of Notch3 mutations, MRI features and founder effect of CADASIL in Chinese. *J Neurol* **256**:249–255.
73. Lesnik Oberstein SA, van den Boom R, van Buchem MA, van Houwelingen HC, Bakker E, Vollebregt E *et al* (2001) Cerebral microbleeds in CADASIL. *Neurology* **57**:1066–1070.
74. Lesnik Oberstein SA, Jukema JW, van Duinen SG, Macfarlane PW, van Houwelingen HC, Breuning MH *et al* (2003) Myocardial infarction in cerebral autosomal dominant arteriopathy with subcortical infarcts and leukoencephalopathy (CADASIL). *Medicine* **82**:251–256.
75. Lian L, Li D, Xue Z, Liang Q, Xu F, Kang H *et al* (2013) Spontaneous intracerebral hemorrhage in CADASIL. *J Headache Pain* **14**:98.
76. Liebetrau M, Herzog J, Kloss CU, Hamann GF, Dichgans M (2002) Prolonged cerebral transit time in CADASIL: a transcranial ultrasound study. *Stroke* **33**:509–512.
77. Liem MK, van der Grond J, Haan J, van den Boom R, Ferrari MD, Knaap YM *et al* (2007) Lacunar infarcts are the main correlate with cognitive dysfunction in CADASIL. *Stroke* **38**:923–928.
78. Liem MK, Lesnik Oberstein SA, Vollebregt MJ, Middelkoop HA, van der Grond J, Helderman-van den Enden AT (2008) Homozygosity for a Notch3 mutation in a 65-year-old CADASIL

patient with mild symptoms: a family report. *J Neurol* **255**:1978–1980.
79. Logeat F, Bessia C, Brou C, LeBail O, Jarriault S, Seidah NG, Israel A (1998) The Notch1 receptor is cleaved constitutively by a furin-like convertase. *Proc Natl Acad Sci U S A* **95**:8108–8112.
80. Low WC, Santa Y, Takahashi K, Tabira T, Kalaria RN (2006) CADASIL-causing mutations do not alter Notch3 receptor processing and activation. *Neuroreport* **17**:945–949.
81. Maeda S, Nakayama H, Isaka K, Aihara Y, Nemoto S (1976) Familial unusual encephalopathy of Binswanger's type without hypertension. *Folia Psychiatr Neurol Jpn* **30**:165–177.
82. Mazzei R, Guidetti D, Ungaro C, Conforti FL, Muglia M, Cenacchi G *et al* (2008) First evidence of a pathogenic insertion in the NOTCH3 gene causing CADASIL. *J Neurol Neurosurg Psychiatry* **79**:108–110.
83. Mendioroz M, Fernández-Cadenas I, Del Río-Espinola A, Rovira A, Solé E, Fernández-Figueras MT *et al* (2010) A missense HTRA1 mutation expands CARASIL syndrome to the Caucasian population. *Neurology* **75**:2033–2035.
84. Miao Q, Paloneva T, Tuominen S, Pöyhönen M, Tuisku S, Viitanen M *et al* (2004) Fibrosis and stenosis of the long penetrating cerebral arteries: the cause of the white matter pathology in cerebral autosomal dominant arteriopathy with subcortical infarcts and leukoencephalopathy. *Brain Pathol* **14**:358–364.
85. Miao Q, Kalimo H, Bogdanovic N, Kostulas K, Börjesson-Hanson A, Viitanen M (2006) Cerebral arteriolar pathology in a 32-year-old patient with CADASIL. *Neuropathol Appl Neurobiol* **32**:455–458.
86. Miao Q, Paloneva T, Tuisku S, Roine S, Pöyhönen M, Viitanen M, Kalimo H (2006) Arterioles of the lenticular nucleus in CADASIL. *Stroke* **37**:2242–2247.
87. Mizuno T, Muranishi M, Torugun T, Tango H, Nagakane Y, Kudeken T *et al* (2008) Two Japanese CADASIL families exhibiting Notch3 mutation R75P not involving cysteine residue. *Intern Med* **47**:2067–2072.
88. Moccia M, Penco S, Barone P (2014) Letter by Moccia et al regarding article "Archetypal Arg169Cys mutation in Notch3 does not drive the pathogenesis in cerebral autosomal dominant arteriopathy with subcortical infarcts and leucoencephalopathy via a loss-of-function mechanism". *Stroke* **45**:e128.
89. Monet M, Domenga V, Lemaire B, Souilhol C, Langa F, Babinet C *et al* (2007) The archetypal R90C CADASIL-*NOTCH3* mutation retains Notch3 function in vivo. *Hum Mol Genet* **16**:982–992.
90. Monet-Leprêtre M, Bardot B, Lemaire B, Domenga V, Godin O, Dichgans M *et al* (2009) Distinct phenotypic and functional features of CADASIL mutations in the Notch3 ligand binding domain. *Brain* **132**:1601–1612.
91. Monet-Leprêtre M, Haddad I, Baron-Menguy C, Fouillot-Panchal M, Riani M, Domenga-Denier V *et al* (2013) Abnormal recruitment of extracellular matrix proteins by excess Notch3 ECD: a new pathomechanism in CADASIL. *Brain* **136**:1830–1845.
92. Morroni M, Marzioni D, Ragno M, Di Bella P, Cartechini E, Pianese L *et al* (2013) Role of electron microscopy in the diagnosis of CADASIL syndrome: a study of 32 patients. *PLoS ONE* **8**:e65482.
93. Mykkänen K, Savontaus ML, Juvonen V, Sistonen P, Tuisku S, Tuominen S *et al* (2004) Detection of the founder effect in Finnish CADASIL families. *Eur J Hum Genet* **12**:813–819.
94. Mykkänen K, Junna M, Amberla K, Bronge L, Kääriäinen H, Pöyhönen M *et al* (2009) Different clinical phenotypes in monozygotic CADASIL twins with a novel *NOTCH3* mutation. *Stroke* **40**:2215–2218.
95. Narayan SK, Gorman G, Kalaria RN, Ford GA, Chinnery PF (2012) The minimum prevalence of CADASIL in northeast England. *Neurology* **78**:1025–1027.
96. Nichols JT, Miyamoto A, Olsen SL, D'Souza B, Yao C, Weinmaster G (2007) DSL ligand endocytosis physically dissociates Notch1 heterodimers before activating proteolysis can occur. *J Cell Biol* **176**:445–458.
97. Nozaki H, Nishizawa M, Onodera O (2014) Features of Cerebral Autosomal Recessive Arteriopathy With Subcortical Infarcts and Leukoencephalopathy. *Stroke* Aug 12. pii: STROKEAHA.114.004236. [Epub ahead of print]
98. Olzscha H, Schermann SM, Woerner AC, Pinkert S, Hecht MH, Tartaglia GG *et al* (2011) Amyloid-like aggregates sequester numerous metastable proteins with essential cellular functions. *Cell* **144**:67–78.
99. Pantoni L, Garcia JH, Gutierrez JA (1996) Cerebral white matter is highly vulnerable to ischemia. *Stroke* **27**:1641–1646.
100. Peters N, Opherk C, Zacherle S, Capell A, Gempel P, Dichgans M (2004) CADASIL-associated Notch3 mutations have differential effects both on ligand binding and ligand-induced Notch3 receptor signaling through RBP-Jκ. *Exp Cell Res* **299**:454–464.
101. Peters N, Opherk C, Danek A, Ballard C, Herzog J, Dichgans M (2005) The pattern of cognitive performance in CADASIL: a monogenic condition leading to subcortical ischemic vascular dementia. *Am J Psychiatry* **162**:2078–2085.
102. Peters N, Freilinger T, Opherk C, Pfefferkorn T, Dichgans M (2007) Effects of short term atorvastatin treatment on cerebral hemodynamics in CADASIL. *J Neurol Sci* **260**:100–105.
103. Prakash N, Hansson E, Betsholtz C, Mitsiadis T, Lendahl U (2002) Mouse Notch3 expression in the pre- and postnatal brain: relationship to the stroke and dementia syndrome CADASIL. *Exp Cell Res* **278**:31–44.
104. Ragno M, Pianese L, Morroni M, Cacchiò G, Manca A, Di Marzio F *et al* (2013) CADASIL coma in an Italian homozygous CADASIL patient: comparison with clinical and MRI findings in age-matched heterozygous patients with the same G528C Notch3 mutation. *Neurol Sci* **34**:1947–1953.
105. Razvi SS, Davidson R, Bone I, Muir KW (2005) The prevalence of cerebral autosomal dominant arteriopathy with subcortical infarcts and leucoencephalopathy (CADASIL) in the west of Scotland. *J Neurol Neurosurg Psychiatry* **76**:739–741.
106. Reyes S, Viswanathan A, Godin O, Dufouil C, Benisty S, Hernandez K (2009) Apathy: a major symptom in CADASIL. *Neurology* **72**:905–910.
107. Rinnoci V, Nannucci S, Valenti R, Donnini I, Bianchi S, Pescini F *et al* (2013) Cerebral hemorrhages in CADASIL: report of four cases and a brief review. *J Neurol Sci* **330**:45–51.
108. Roine S, Pöyhönen M, Timonen S, Tuisku S, Marttila R, Sulkava R *et al* (2005) Neurologic symptoms are common during gestation and puerperium in CADASIL. *Neurology* **64**:1441–1443.
109. Roine S, Harju M, Kivelä TT, Pöyhönen M, Nikoskelainen E, Tuisku S *et al* (2006) Ophthalmologic findings in cerebral autosomal dominant arteriopathy with subcortical infarcts and leukoencephalopathy: a cross-sectional study. *Ophthalmology* **113**:1411–1417.
110. Ruchoux MM, Guerouaou D, Vandenhaute B, Pruvo JP, Vermersch P, Leys D (1995) Systemic vascular smooth muscle cell impairment in cerebral autosomal dominant arteriopathy with subcortical infarcts and leukoencephalopathy. *Acta Neuropathol* **89**:500–512.
111. Ruchoux MM, Domenga V, Brulin P, Maciaze J, Limol S, Tournier-Lasserve E *et al* (2003) Transgenic mice expressing mutant Notch3 develop vascular alterations characteristic of cerebral autosomal dominant arteriopathy with subcortical infarcts and leukoencephalopathy. *Am J Pathol* **162**:329–342.

112. Saiki S, Sakai K, Saiki M, Kitagawa Y, Umemori T, Murata K *et al* (2006) Varicose veins associated with CADASIL result from a novel mutation in the *NOTCH3* gene. *Neurology* **67**:337–339.
113. Salomon N (2014) Neuroimaging of small vessel disease. *Brain Pathol*.
114. Scholefield J, Watson L, Smith D, Greenberg J, Wood MJ (2014) Allele-specific silencing of mutant Ataxin-7 in SCA7 patient-derived fibroblasts. *Eur J Hum Genet* doi: 10.1038/ejhg.2014.39; Mar 26, [Epub ahead of print].
115. Shibata M (2012) [Clinical manifestations and neuroradiological findings of CARASIL with a novel mutation]. *Rinsho Shinkeigaku* **52**:1363–1364, (Article in Japanese).
116. Shiga A, Nozaki H, Yokoseki A, Nihonmatsu M, Kawata H, Kato T *et al* (2011) Cerebral small-vessel disease protein HTRA1 controls the amount of TGF-β1 via cleavage of proTGF-β1. *Hum Mol Genet* **20**:1800–1810.
117. Singhal S, Bevan S, Barrick T, Rich P, Markus HS (2004) The influence of genetic and cardiovascular risk factors on the CADASIL phenotype. *Brain* **127**:2031–2038.
118. Soong BW, Liao YC, Tu PH, Tsai PC, Lee IH, Chung CP, Lee YC (2013) A homozygous Notch3 mutation p.R544C and a heterozygous TREX1 variant p.C99MfsX3 in a family with hereditary small vessel disease of the brain. *J Chin Med Assoc* **76**:319–324.
119. Stenborg A, Kalimo H, Viitanen M, Terent A, Lind L (2007) Impaired endothelial function of forearm resistance arteries in CADASIL patients. *Stroke* **38**:2692–2697.
120. Taillia H, Chabriat H, Kurtz A, Verin M, Levy C, Vahedi K *et al* (1998) Cognitive alterations in non-demented CADASIL patients. *Cerebrovasc Dis* **8**:97–101.
121. Tang SY, Alliston T (2013) Regulation of postnatal bone homeostasis by TGFβ. *Bonekey Rep* **2**:255. doi: 10.1038/bonekey.2012.255
122. Tikka S, Mykkänen K, Ruchoux MM, Bergholm R, Junna M, Pöyhönen M *et al* (2009) Congruence between *NOTCH3* mutations and GOM in 131 CADASIL patients. *Brain* **132**:933–939.
123. Tikka S, Ng YP, Di Maio G, Mykkänen K, Siitonen M, Lepikhova T *et al* (2012) CADASIL mutations and shRNA silencing of Notch3 affect actin organization in cultured vascular smooth muscle cells. *J Cereb Blood Flow Metab* **32**:2171–2180.
124. Todorovic V, Rifkin DB (2012) LTBPs, more than just an escort service. *J Cell Biochem* **113**:410–418.
125. Tournier-Lasserve E, Joutel A, Melki J *et al* (1993) Cerebral autosomal dominant arteriopathy with subcortical infarcts and leukoencephalopathy maps to chromosome 19q12. *Nat Genet* **3**:256–259.
126. Tuominen S, Juvonen V, Amberla K, Jolma T, Rinne JO, Tuisku S *et al* (2001) Phenotype of a homozygous CADASIL patient in comparison to 9 age-matched heterozygous patients with the same R133C Notch3 mutation. *Stroke* **32**:1767–1774.
127. Tuominen S, Miao Q, Kurki T, Tuisku S, Pöyhönen M, Kalimo H *et al* (2004) Positron emission tomography examination of cerebral blood flow and glucose metabolism in young CADASIL patients. *Stroke* **35**:1063–1067.
128. van Bogaert L (1955) Encephalopathie sous-corticale progressive (Binswanger) a evolution rapide sous deuz soeurs. *Med Hellen* **24**:961–972.
129. Verin M, Rolland Y, Landgraf F, Chabriat H, Bompais B, Michel A *et al* (1995) New phenotype of the cerebral autosomal dominant arteriopathy mapped to chromosome 19: migraine as the prominent clinical feature. *J Neurol Neurosurg Psychiatry* **59**:579–585.
130. Vinciguerra C, Rufa A, Bianchi S, Sperduto A, De Santis M, Malandrini A *et al* (2014) Homozygosity and severity of phenotypic presentation in a CADASIL family. *Neurol Sci* **35**:91–93.
131. Wang XL, Li CF, Guo HW, Cao BZ (2012) A novel mutation in the HTRA1 gene identified in Chinese CARASIL pedigree. *CNS Neurosci Ther* **18**:867–869.
132. Wang Z, Yuan Y, Zhang W, Lv H, Hong D, Chen B *et al* (2011) Notch3 mutations and clinical features in 33 mainland Chinese families with CADASIL. *J Neurol Neurosurg Psychiatry* **82**:534–539.
133. Watanabe M, Adachi Y, Jackson M, Yamamoto-Watanabe Y, Wakasaya Y *et al* (2012) An unusual case of elderly onset cerebral autosomal dominant arteriopathy with subcortical infarcts and leukoencephalopathy (CADASIL) with multiple cerebrovascular risk factors. *J Stroke Cerebrovasc Dis* **21**:143–145.
134. Watanabe-Hosomi A, Watanabe Y, Tanaka M, Nakagawa M, Mizuno T (2012) Transendocytosis is impaired in CADASIL-mutant Notch3. *Exp Neurol* **233**:303–311.
135. Yamamoto Y, Craggs LJ, Watanabe A, Booth T, Attems J, Low RW *et al* (2013) Brain microvascular accumulation and distribution of the Notch3 ectodomain and granular osmiophilic material in CADASIL. *J Neuropathol Exp Neurol* **72**:416–431.
136. Yanagawa S, Ito N, Arima K, Ikeda S (2002) Cerebral autosomal recessive arteriopathy with subcortical infarcts and leukoencephalopathy. *Neurology* **58**:817–820.